

**Deforming, revolving and resolving - New paths in the
string theory landscape**

**Diego CHIALVA, Ulf DANIELSSON, Niklas JOHANSSON,
Magdalena LARFORS and Marcel VONK**



Institut des Hautes Études Scientifiques
35, route de Chartres
91440 – Bures-sur-Yvette (France)

Octobre 2007

IHES/P/07/33

Deforming, revolving and resolving

New paths in the string theory landscape

Diego Chialva^{1,a}, Ulf H. Danielsson^{2,a}, Niklas Johansson^{3,a},
Magdalena Larfors^{4,a} and Marcel Vonk^{5,b}

^aInstitutionen för Teoretisk Fysik, Box 803, SE-751 08 Uppsala, Sweden.

^bIHÉS, Le Bois-Marie, 35, route de Chartres, F-91440 Bures-sur-Yvette, France.

¹diego.chialva@teorfys.uu.se

²ulf.danielsson@teorfys.uu.se

³niklas.johansson@teorfys.uu.se

⁴magdalena.larfors@teorfys.uu.se

⁵mail@marcelvonk.nl

Abstract

In this paper we investigate the properties of series of vacua in the string theory landscape. In particular, we study minima to the flux potential in type IIB compactifications on the mirror quintic. Using geometric transitions, we embed its one dimensional complex structure moduli space in that of another Calabi–Yau with $h^{1,1} = 86$ and $h^{2,1} = 2$. We then show how to construct infinite series of continuously connected minima to the mirror quintic potential by moving into this larger moduli space, applying its monodromies, and moving back. We provide an example of such series, and discuss their implications for the string theory landscape.

October 2007

1 Introduction

Compactifications of string theory on six-dimensional internal manifolds provide four-dimensional low-energy effective field theories that could describe our world. (See e.g. [1].) Since these models originate from string theory, there is a consistent way of completing them into theories of quantum gravity. However, there is an enormous number of such compactifications. Even if we restrict the internal manifold to be a (conformally) Calabi–Yau threefold the number of possibilities is huge. Furthermore, compactifying string theory on a specific Calabi–Yau leads to a *family* of four-dimensional theories, since the moduli of the manifold are unfixed.¹ Thus the size and shape of the manifold can fluctuate both over three-dimensional space and time. The latter can lead to dynamical problems, such as a rapid decompactification of the theory.

One way to fix the moduli of the manifold is to introduce fluxes, that pierce certain non-trivial cycles of the manifold.² In type IIB these fluxes will create a potential for the complex structure moduli of the Calabi–Yau [3]. In order to fix the Kähler moduli we need to take quantum corrections of the theory into account [4, 5]. These effects trap the moduli in metastable minima of the resulting potential, thus stabilizing the compactification. The result is a metastable four-dimensional effective field theory, also known as a string theory vacuum. Each vacuum corresponds to a particular choice of internal manifold, moduli and fluxes. The large number of such vacua form the string theory landscape [6].³

A landscape of string theory vacua has many implications for the four-dimensional physics of our world. Some consequences are universal, such as the non-uniqueness and metastability of universes. Other consequences for four-dimensional physics depend on the topography of the landscape, i.e. the distribution of vacua in parameter space, the height and width of potential barriers between vacua, whether the landscape is smooth or rough etc. This will determine the probability for tunneling between vacua, and thus the life-time and evolution of a universe that is described by one vacuum in the landscape. The topographic properties of the landscape are also important for the selection of a particular vacuum, and the computability problems related to this [7, 8, 9].

Mapping out the entire string theory landscape is an enormously difficult task. The landscape is parametrized by a large number of continuous fields and discrete fluxes, and it is difficult to find a systematic way to describe the potential between vacua. However, we can ask ourselves if we can construct models for (parts of) the landscape, and what we can learn from such models. Examples of such considerations

¹Often, when we speak of “a Calabi-Yau threefold”, what we really mean is a family of Calabi-Yau threefolds. These threefolds are topologically equivalent, but their shapes and sizes differ, as specified by their complex structure and Kähler moduli.

²See [2] for a nice review on flux compactifications.

³Compactifications of other string theories also yield vacua in the landscape. To be precise, we should note that introducing branes in the compactifications also yields new vacua.

include [10, 11, 12, 13]. In particular, in [14], it was found that the potential created by three-fluxes in type IIB compactifications often has series of minima that are connected by continuous paths in complex structure moduli space. The construction of such series was based on the use of monodromy transformations.

More specifically, by moving around singular points in the complex structure moduli space, monodromies transform the three-cycles pierced by fluxes. This is equivalent to changing the flux and keeping the cycles fixed. Thus it is possible to move continuously between different minima of the potential, corresponding to different discrete flux values, and still have full control over the potential. Some explicit examples of such series were computed numerically for the mirror quintic, yielding a complete picture of the barriers between minima in this model landscape.

However, we cannot resolve the barriers between all minima. Not all flux configurations — and hence not all minima of the potential — are connected by monodromy transformations. This suggests a subdivision of the landscape into several islands. Only minima on the same island are connected by continuous paths in complex structure moduli space.

In the analysis of [14] some questions remained open. The first concerned the length of the series. Although only finite series of continuously connected minima were found, there was no general argument as to why infinite series should not exist.⁴ One way of indirectly proving the existence of infinite connected series, relates to an interesting mathematical question. The monodromy transformations of the mirror quintic form a subgroup of $Sp(4, \mathbb{Z})$ so only islands connected by such transformations can possibly be connected by monodromies. Furthermore, there are infinite series connected by $Sp(4, \mathbb{Z})$ transformations [14]. This means that if the index of the monodromy group is finite in $Sp(4, \mathbb{Z})$ — meaning that the number of islands connected by symplectic transformations are finite — then there are infinite series connected by monodromy transformations. Unfortunately, it is not known whether this index is finite or not [15].

Another question was whether these islands in the landscape really exist, or if they are only an artifact of modeling too small a part of the landscape. In this paper we introduce a new way of computing potential barriers between string theory vacua. We follow new paths that take us to other parts of the landscape. These paths go via topology changing transitions of the internal manifold.

It is well known that many Calabi–Yau manifolds are connected through geometric transitions [16, 17]. E.g., as we will discuss below, it is reasonable to assume that the mirror quintic, $\mathcal{M}_{(101,1)}$, is connected to a Calabi–Yau threefold with two complex

⁴Note that we are only studying minima of the potential created by fluxes. When we discuss the length of the series of minima we disregard the fixing of Kähler moduli, which, in e.g. the KKLT model [4], depends on the magnitude of the fluxes. For the sake of argument, we will also disregard questions about back-reaction of the fluxes on the manifold (see e.g. [2] and references therein). Even though these effects would probably cut off the series of vacua in the string theory landscape at finite length, we expect the remaining series to be long. Hence there are interesting topographic features, such as many closely spaced vacua, in the string theory landscape if these infinite series of minima exist.

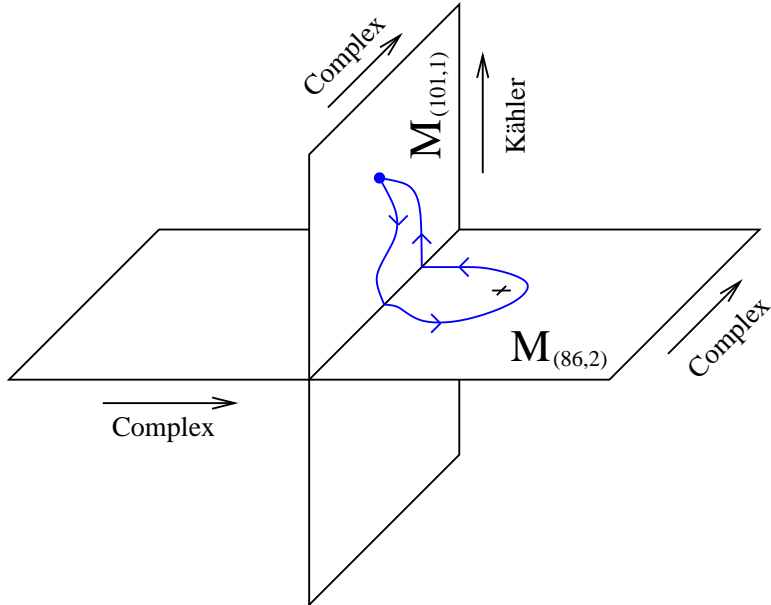


Figure 1: *The two moduli spaces near the geometric transition. The intersection of the two planes represents the moduli space of the singular manifold, which has 86 remaining Kähler moduli and 1 remaining complex structure modulus. Blowing up two-cycles turns the singular manifold into a nonsingular mirror quintic, moving it in its Kähler moduli space. Blowing up three-cycles turns the singular manifold into a nonsingular $\mathcal{M}_{(86,2)}$, moving it in its complex structure moduli space. Note that in particular, we can think of the complex structure moduli space $M_{(101,1)}$ of the mirror quintic as a submanifold of the complex structure moduli space $M_{(86,2)}$ of $\mathcal{M}_{(86,2)}$.*

structure moduli and 86 Kähler moduli, $\mathcal{M}_{(86,2)}$, through a so-called conifold, or geometric, transition. Thus, we can view the complex structure moduli space of the mirror quintic as a subspace of the moduli space of the other Calabi–Yau. It is possible to make excursions into this larger space and use its monodromies to find continuous paths between minima on the mirror quintic.

To reach the singular point where the conifold transition can happen we need to move in the Kähler moduli space of the mirror quintic, as shown in figure 1. It follows that the paths between the minima will go through both the Kähler moduli space of the mirror quintic and the complex structure moduli space of $\mathcal{M}_{(86,2)}$. In this way, we get new continuous paths between minima in our model landscape. If we have a good description of the potential on both the Kähler and the complex structure moduli spaces, we get a complete description of the potential barriers between minima.

This paper will probe deeper into the topography of this model landscape, by extending the complex structure moduli space of the mirror quintic using conifold transitions as described above. To do this, we first compute the geometric data of the Calabi–Yau $\mathcal{M}_{(86,2)}$ using toric geometry (section 2). In section 3 we compute

the periods and monodromies of $\mathcal{M}_{(86,2)}$ and in section 4 we show how the complex structure moduli space of $\mathcal{M}_{(101,1)}$ is embedded in the moduli space of $\mathcal{M}_{(86,2)}$. The geometric transition between $\mathcal{M}_{(86,2)}$ and $\mathcal{M}_{(101,1)}$, with and without fluxes, is discussed in section 5. In section 6, we give an explicit example of a continuously connected series of minima and provide an example of an infinite series. Conventions and a recapitulation of Calabi–Yau geometry are given in appendix A.

2 Toric description of $\mathcal{M}_{(86,2)}$

In this paper, we are interested in continuous deformations of the periods of the mirror quintic. In particular, we want to study how these periods depend on the coordinates of the complex structure moduli space.

The mirror quintic $\mathcal{M}_{(101,1)}$, with Hodge numbers $h^{1,1} = 101$ and $h^{2,1} = 1$, is related through mirror symmetry [18, 19] to the quintic in \mathbb{P}^4 , which has $h^{1,1} = 1$ and $h^{2,1} = 101$. The quintic itself is furthermore known to be connected [17, 20] to a manifold of Hodge numbers $h^{1,1} = 2$ and $h^{2,1} = 86$ through a geometric transition.⁵ It is therefore natural to expect that the mirror of this process also occurs⁶ and that the mirror quintic has a geometric transition to a Calabi–Yau threefold $\mathcal{M}_{(86,2)}$ with Hodge numbers

$$h^{1,1} = 86, \quad h^{2,1} = 2. \quad (1)$$

We will see below that mirror symmetry indeed suggests a natural candidate for this manifold.

We will exploit the above relations between moduli spaces to find very general continuous deformations of the periods of the mirror quintic. In particular we will be interested in the behavior of the periods under the geometric transition between the mirror quintic and the manifold $\mathcal{M}_{(86,2)}$. In order to construct the manifold and calculate the periods and their behavior under these deformations, we will use the tools of *toric geometry*.

2.1 Toric Geometry for Calabi–Yau manifolds

It is possible to construct Calabi–Yau manifolds as the common zero locus of a set of polynomials defined on a toric variety. In this subsection we will briefly review

⁵When two families of Calabi–Yau manifolds are related by a geometric transition their moduli spaces are connected through some loci where the manifolds are singular. The geometric transition can be understood as the shrinking of some three-spheres and the successive blowing up of the resulting singularities into two-spheres. The simplest example of this behavior is the transition between resolved and deformed conifolds. See section 5 for a more complete discussion.

⁶As far as we are aware, there is no mathematical theorem claiming that the mirror of a geometric transition is again a geometric transition. However, this has been suggested to be true in several explicit cases, see e. g. [27]. In the present case, we will see explicitly how the complex structure moduli space of the mirror quintic can be embedded in that of $\mathcal{M}_{(86,2)}$.

how to obtain these equations and the embedding toric variety using polytopes of lattice points. The data encoded in these points are useful to define a suitable set of coordinates on the complex structure moduli space, and to compute the periods of the Calabi–Yau threefold (see section 3). Moreover, the defining equations for the mirror of a Calabi–Yau can be represented through another polytope related to the original one, following a method by V. Batyrev [21]. In this subsection we will state the general procedure and define the basic concepts in order to understand it. Readers not well-versed in toric geometry might want to consult [22, 23, 24, 25, 26].

A d -dimensional toric variety X can be constructed as a quotient $X = \frac{(\mathbb{C}^*)^{n-Z}}{G}$, where G is an m -dimensional group, and $d = n - m$. It contains the complex torus $(\mathbb{C}^*)^d$ as an open subset in such a way that the action of the torus on itself, given by the group structure, extends to the whole of X .

We can either study the toric variety using a set of affine coordinates $\{t_i, i = 1 \dots d\}$, corresponding to coordinates on the torus $(\mathbb{C}^*)^d$, or with a set of homogeneous ones $\{x_j, j = 1 \dots n\}$ describing the entire manifold. Using either of these coordinate sets, we can construct a set of monomials that form the building blocks for the defining equations of the Calabi–Yau. In this paper, we will mainly use the affine coordinates.

Let us first discuss the case where the Calabi–Yau manifold is defined through a single equation. A convenient way to encode monomials is by points in a lattice. Every monomial of the form

$$\prod_{i=1}^d t_i^{m_i} \equiv t^{\mathbf{m}} \quad (2)$$

is represented by a vector of exponents \mathbf{m} in some lattice $M \cong \mathbb{Z}^d$. More generally, a polytope $\Delta \subset M$ describes a set of monomials. The vector space given by all the linear combinations of such monomials is known as the space of *Laurent polynomials* associated to the polytope Δ . A Laurent polynomial belonging to this space therefore has the form

$$\mathbf{L}(\{t_i\}) = \sum_l a_l t^{\mathbf{m}_l}, \quad \mathbf{m}_l \in \Delta. \quad (3)$$

The set of homogeneous coordinates is defined as follows: given a polytope $\Delta \subset M$, we can define its dual, or polar, polytope as

$$\Delta^\circ = \{\mathbf{n} \in N \mid \langle \mathbf{m}, \mathbf{n} \rangle \geq -1, \forall \mathbf{m} \in \Delta\}. \quad (4)$$

Here, $N \cong \mathbb{Z}^d$ is the lattice dual to M . With a simplified notation we can write:

$$\langle \Delta^\circ, \Delta \rangle \geq -1. \quad (5)$$

To every vertex \mathbf{n}_j of this polytope we can associate a homogeneous coordinate x_j . The two sets of coordinates are then related by the equations

$$t_i = \prod_{j=1}^d x_j^{\langle \mathbf{e}_i, \mathbf{n}_j \rangle} \quad (6)$$

where \mathbf{e}_i , are the basis vectors of M . Using this relation, starting from the Laurent monomials we can define the set of monomials in the homogeneous coordinates x_j that are invariant under the group G appearing in the quotient construction of the toric variety.

As a side remark, we note that the lattice N is often taken as the starting point for the construction of a toric variety. The *fan* Σ describing the toric variety is a collection of cones in $\mathbb{R}^d \supset N$. The cones of Σ are spanned by the faces of Δ° . In particular, there is a one-to-one relation among the one-dimensional cones, the vertices of Δ° and the homogeneous coordinates. Thus, a polytope Δ contains all the information we need⁷ to construct a toric variety, which we therefore denote by X_Δ .

We have now collected all the ingredients: the zero locus of the Laurent polynomials (or their homogenization through (6)) of Δ defines a Calabi–Yau manifold⁸ inside the toric variety X_Δ . If Δ is *reflexive*, meaning roughly that it contains the origin as its only interior point, the Laurent polynomials that we can instead obtain from the dual polytope Δ° define its mirror manifold. This result is the mirror construction of V. Batyrev [21].

Above, we have described a Calabi–Yau manifold as a hypersurface defined by a single polynomial, but we can also study the complete⁹ intersection of several hypersurfaces. In this case, a refined construction is necessary [29, 30, 31, 32]. Once again, the data of the manifold are encoded in a lattice polytope, but now this polytope is appropriately partitioned into a set of sub-polytopes¹⁰:

$$\Delta = \sum_k \Delta_k \tag{7}$$

Every sub-polytope will encode the data of one of the defining Laurent polynomials for the Calabi–Yau. This time, its mirror manifold is obtained from a related polytope and a corresponding partition:

$$\nabla = \sum_k \nabla_k. \tag{8}$$

The sub-polytopes ∇_k are given by

$$\nabla_k = \text{Conv}(\{0\} \cup \Xi_k), \quad \langle \nabla_k, \Delta_{k'} \rangle \geq -\delta_{k,k'}. \tag{9}$$

where, the round brackets indicate the convex hull and the Ξ_k are defined as a partition of the vertices of the dual polytope Δ° for Δ such that:

$$\Delta^\circ = \text{Conv}\left(\bigcup_k \Xi_k\right). \tag{10}$$

⁷In fact, to make the variety smooth, in certain cases one needs a triangulation or a refinement of Δ° with additional vertices. We will not go into these details here.

⁸For the conditions on when the manifold is indeed Calabi–Yau, see e. g. [21].

⁹The completeness condition is a certain regularity condition; see [28] for details.

¹⁰The relevant sum here and in (8) is the Minkowski sum, and the partition must be a so-called *nef partition* [31, 32]. The term *nef* (“numerically effective”) basically means that when shifted appropriately, the constituent polytopes intersect only in the origin.

In the next subsection, we will explicitly construct the nef partition $\{\Delta_k\}$ for the manifold $\mathcal{M}_{(86,2)}$ of our interest. It is evident from the description above that, ∇ and Δ being mirror to each other, we can start the construction of the mirror pair from an assigned polytope ∇ . In this case we will partition its dual as:

$$\nabla^\circ = \text{Conv}\left(\bigcup_k E_k\right), \quad (11)$$

where $\langle \exists_k, E_{k'} \rangle \geq -\delta_{k,k'}$, and from this, just as above, we will obtain:

$$\Delta_k = \text{Conv}(\{0\} \cup E_k), \quad (12)$$

which we are eventually interested in.

2.2 Toric data for $\mathcal{M}_{(86,2)}$

In order to obtain and list the data for the manifold $\mathcal{M}_{(86,2)}$, it is convenient to start from those of its mirror, which we denote $\mathcal{W}_{(2,86)}$. Therefore, we obtain the polytope Δ and its nef partition $\{\Delta_k\}$ relevant for $\mathcal{M}_{(86,2)}$, starting from its mirror ∇ and the nef partition for $\mathcal{W}_{(2,86)}$. A useful tool in performing the calculations below is the package PALP [33].

A well-known way [17, 34] to describe the manifold $\mathcal{W}_{(2,86)}$ is as a complete intersection of two hypersurfaces given by equations of degree $(1, 4)$ and $(1, 1)$ in $\mathbb{P}^1 \times \mathbb{P}^4$.

These equations can be described by the polytope and the nef partition¹¹

$$\nabla = \nabla_1 + \nabla_2 \quad (13)$$

where¹²

$$\nabla_1 = \text{Conv} \begin{pmatrix} -1 & 0 & -1 & -1 & -1 \\ -1 & 4 & -1 & -1 & -1 \\ -1 & 0 & 3 & -1 & -1 \\ -1 & 0 & -1 & 3 & -1 \\ -1 & 0 & -1 & -1 & 3 \\ 0 & 0 & -1 & -1 & -1 \\ 0 & 4 & -1 & -1 & -1 \\ 0 & 0 & 3 & -1 & -1 \\ 0 & 0 & -1 & 3 & -1 \\ 0 & 0 & -1 & -1 & 3 \end{pmatrix}, \quad \nabla_2 = \text{Conv} \begin{pmatrix} 0 & -1 & 0 & 0 & 0 \\ 0 & 0 & 0 & 0 & 0 \\ 0 & -1 & 1 & 0 & 0 \\ 0 & -1 & 0 & 1 & 0 \\ 0 & -1 & 0 & 0 & 1 \\ 1 & -1 & 0 & 0 & 0 \\ 1 & 0 & 0 & 0 & 0 \\ 1 & -1 & 1 & 0 & 0 \\ 1 & -1 & 0 & 1 & 0 \\ 1 & -1 & 0 & 0 & 1 \end{pmatrix}.$$

and therefore:

$$\nabla = \text{Conv} \begin{pmatrix} -1 & -1 & -1 & -1 & -1 \\ -1 & 4 & -1 & -1 & -1 \\ -1 & -1 & 4 & -1 & -1 \\ -1 & -1 & -1 & 4 & -1 \\ -1 & -1 & -1 & -1 & 4 \\ 1 & -1 & -1 & -1 & -1 \\ 1 & 4 & -1 & -1 & -1 \\ 1 & -1 & 4 & -1 & -1 \\ 1 & -1 & -1 & 4 & -1 \\ 1 & -1 & -1 & -1 & 4 \end{pmatrix}.$$

∇_1 and ∇_2 intersect only in the origin and hence form a nef partition of ∇ .

¹¹To describe the equations, we could have taken any shifted version of these polytopes. This particular choice is made in order to obtain convenient polynomials in the following subsection.

¹²Convention: the vertices are written as the rows of the matrix.

The dual polytope of ∇ , as explained in the previous subsection, is given by:

$$\nabla^\circ = \text{Conv} \left(\begin{array}{ccccc} 1 & 0 & 0 & 0 & 0 \\ -1 & 0 & 0 & 0 & 0 \\ 0 & 1 & 0 & 0 & 0 \\ 0 & 0 & 1 & 0 & 0 \\ 0 & 0 & 0 & 1 & 0 \\ 0 & 0 & 0 & 0 & 1 \\ 0 & -1 & -1 & -1 & -1 \end{array} \right).$$

Its vertices are in correspondence with the fan for $\mathbb{P}^1 \times \mathbb{P}^4$.¹³

By looking at formulas (8, 9, 10), we build the nef partition of the polytope related to the $\mathcal{M}_{(86,2)}$. First we subdivide the set E of vertices of ∇° in two sets $E = E_1 \cup E_2$:

$$\begin{aligned} E_1 &= \{(1, 0, 0, 0, 0), (0, 0, 1, 0, 0), (0, 0, 0, 1, 0), (0, 0, 0, 0, 1), (0, -1, -1, -1, -1)\} \\ E_2 &= \{(-1, 0, 0, 0, 0), (0, 1, 0, 0, 0)\}. \end{aligned} \quad (14)$$

such that $\langle E_k, \nabla_{k'} \rangle \geq -\delta_{k,k'}$. The mirror is now constructed by taking the Δ_k to be the convex hulls of $E_k \cup \{0\}$:

$$\Delta_1 = \text{Conv} \left(\begin{array}{ccccc} 0 & 0 & 0 & 0 & 0 \\ 1 & 0 & 0 & 0 & 0 \\ 0 & 0 & 1 & 0 & 0 \\ 0 & 0 & 0 & 1 & 0 \\ 0 & 0 & 0 & 0 & 1 \\ 0 & -1 & -1 & -1 & -1 \end{array} \right), \quad \Delta_2 = \text{Conv} \left(\begin{array}{ccccc} 0 & 0 & 0 & 0 & 0 \\ -1 & 0 & 0 & 0 & 0 \\ 0 & 1 & 0 & 0 & 0 \end{array} \right).$$

To complete the mirror symmetry circle, one can construct the Minkowski sum $\Delta = \Delta_1 + \Delta_2$ (which is a polytope with 16 vertices) and its dual Δ° (which is a polytope with 19 vertices), which spans the fan for the manifold in which $\mathcal{M}_{(86,2)}$ is a complete intersection. As a consistency check, one can then show that the mirror of the mirror is the original manifold. In this paper, we will have no need for the explicit expressions of the further toric data involved, so we omit them here.

2.3 Local equations and Mori generators

As explained previously we can write the defining equation for the complete intersection in homogeneous or affine coordinates. In terms of the affine coordinates, we can conveniently relate each lattice point in the Δ_i to a monomial, and we simply read off the equations:

$$f_1 \equiv 1 - g_1 = 1 - a_1 t_1 - a_2 t_3 - a_3 t_4 - a_4 t_5 - a_5 / t_2 t_3 t_4 t_5 \quad (15)$$

$$f_2 \equiv 1 - g_2 = 1 - a_6 / t_1 - a_7 t_2, \quad (16)$$

where we used the convention of scaling the constant term to 1 and giving all other terms a minus sign. The a_i in these equations are adjustable constants. It turns out that these local equations are enough to determine the periods of the holomorphic three-form on $\mathcal{M}_{(86,2)}$. We do this calculation in section 3.

Varying the a_i changes the complex structure of our manifold. As can be expected from the fact that the moduli space has dimension two, not all of the a_i are moduli:

¹³This fan is simply the direct sum of the fans for \mathbb{P}^1 and \mathbb{P}^4 . It has seven one-dimensional cones: two for \mathbb{P}^1 and five for \mathbb{P}^4 .

only certain combinations of them are. In fact, we will see in the next section that it is the constant terms in the products $g_1^n g_2^m$ that determine the moduli. We can expand every power of g_1 and g_2 , respectively, in Newton binomials, and therefore these constant terms will be given by those powers l_ℓ of the monomials $t^{\mathbf{m}_\ell}$, $\mathbf{m}_\ell \in \Delta_1 \cup \Delta_2$, in g_1, g_2 such that

$$l_\ell \mathbf{m}_\ell = 0, \quad \ell = 1, \dots, |\Delta_1 \cup \Delta_2|. \quad (17)$$

where $|\Delta_1 \cup \Delta_2|$ is the number of points in $\Delta_1 \cup \Delta_2$ (excluding the origin).

It is easy to see that the vectors \mathbf{l} of the coefficients $\{l_\ell\}$ of these relations form a vector space. A convenient choice of basis for this space is

$$\begin{pmatrix} \mathbf{l}^{(1)} \\ \mathbf{l}^{(2)} \end{pmatrix} = \begin{pmatrix} 1 & 0 & 0 & 0 & 0 & 1 & 0 \\ 0 & 1 & 1 & 1 & 1 & 0 & 1 \end{pmatrix}. \quad (18)$$

This basis corresponds to a set of coordinates

$$\phi_k = \prod_{\ell} a_{\ell}^{l_{\ell}^{(k)}} \quad (19)$$

for the complex structure moduli space, that are particularly useful for describing mirror constructions. In our case, in fact, each positive linear combination $ml^{(1)} + nl^{(2)}$ corresponds to a power of $\phi_1^m \phi_2^n$ appearing in some product of g_1 's and g_2 's, where

$$\phi_1 = a_1 a_6, \quad \phi_2 = a_2 a_3 a_4 a_5 a_7. \quad (20)$$

Thus, the cone¹⁴ generated by $\mathbf{l}^{(1)}$ and $\mathbf{l}^{(2)}$ will play a crucial role in calculating the periods of the holomorphic three-form. This cone is called the *Mori cone*, and the $\mathbf{l}^{(i)}$ are called the *Mori generators*.

3 Periods and monodromies of $\mathcal{M}_{(86,2)}$

In this section we put the machinery of toric geometry to work. Our aim is to calculate the periods and monodromies of $\mathcal{M}_{(86,2)}$. The periods are obtained by finding the solutions to a system of partial differential equations – the Picard–Fuchs (PF) equations. Studying the asymptotic behavior of the periods yields two monodromy transformations of $\mathcal{M}_{(86,2)}$.

The methods for computing the periods and monodromies are well-known, but to our knowledge the periods of this particular manifold have not been explicitly computed before. (See however [35].) A reader familiar with this type of computations can skip the derivations and read the results in equations (44)–(46).

¹⁴That is, the linear combinations of $\mathbf{l}^{(1,2)}$ with non-negative coefficients, corresponding to non-negative powers of the monomials.

3.1 The Picard–Fuchs equations

The periods of a Calabi-Yau 3-fold are the “holomorphic volumes” of a basis of 3-cycles C_I ($I = 1, \dots, 2(h^{2,1}+1)$):

$$\Pi_I = \oint_{C_I} \Omega(\phi_i), \quad (21)$$

where $\Omega(\phi_i)$ is the holomorphic 3-form on the manifold, which depends on the complex structure moduli ϕ_i .

The periods must satisfy the Picard–Fuchs (PF) equations, as we now explain. Repeated differentiation of $\Omega(\phi_i)$ gives elements in $H^3 = H^{3,0} \oplus H^{2,1} \oplus H^{1,2} \oplus H^{0,3}$. Since H^3 has finite dimension, some combinations of derivatives of $\Omega(\phi_i)$ must be exact. Thus $L_k \Omega(\phi_i) = d\eta$, where L_k are some differential operators. Integrating over a 3-cycle we find that the periods must fulfill

$$L_k \Pi_I = \oint_{C_I} L_k \Omega(\phi_i) = \oint_{C_I} d\eta = 0. \quad (22)$$

These are the Picard–Fuchs (PF) equations. By solving them, we find the periods.

To derive the PF equations we use a method based on toric geometry, described in [36]. We build a set of differential operators – the generalized hypergeometric Gel’fand–Kapranov–Zelevinski (GKZ) system – from which, by suitable factorization [36, 37], we can extract the PF operators. These will be written in terms of the coordinates ϕ_1, ϕ_2 in equation (20), that were defined starting from the coefficients of the Laurent polynomials (15,16) and the generators of the Mori cone (18).

The differential operators of the GKZ system are also defined from the generators $l^{(k)}$ of the Mori cone [37]:

$$\begin{aligned} \mathcal{L}_k = & \prod_{\alpha=1}^r (l_{\alpha}^{(k)} \theta_k) (l_{\alpha}^{(k)} \theta_k - 1) \dots (l_{\alpha}^{(k)} \theta_k - l_{\alpha}^{(k)} + 1) \\ & - \prod_{\beta=1}^s \left(- \sum_{i=1}^k l_{0\beta}^{(i)} \theta_i \right) \dots \left(- \sum_{i=1}^k l_{0\beta}^{(i)} \theta_i - l_{0\beta}^{(k)} + 1 \right) \phi_k, \end{aligned} \quad (23)$$

where $\theta_k = \phi_k \frac{\partial}{\partial \phi_k}$, r and s are the dimension and the number of the $l^{(k)}$ respectively, and $l_{0\beta}^{(i)} = - \sum_{\alpha} l_{\alpha}^{(i)} |_{E_{\beta}}$.¹⁵ In our example we obtain:

$$\begin{aligned} \mathcal{L}_1 &= \theta_1^2 - (\theta_1 + \theta_2)(\theta_1 + 4\theta_2)\phi_1 \\ \mathcal{L}_2 &= \theta_2^5 - (\theta_1 + \theta_2)(\theta_1 + 4\theta_2)(\theta_1 + 4\theta_2 - 1)(\theta_1 + 4\theta_2 - 2)(\theta_1 + 4\theta_2 - 3)\phi_2. \end{aligned} \quad (24)$$

The periods of $\mathcal{M}_{(86,2)}$ are solutions to the equations $\mathcal{L}_k \omega = 0$, but in general there are other solutions as well [36]. In fact, the monodromy group does not act irreducibly

¹⁵Since we have a nef partition, the sum goes over the $l^{(k)}$ related to the vertices in E_{β} . See [37].

on the solutions of the GKZ system, as it should do on the periods [37]. To get rid of the false solutions, we factorize [36, 37] the differential operators as

$$\begin{aligned} L_1 &= \mathcal{L}_1 \\ p_1 L_2 &= \mathcal{L}_2 - p_3 \mathcal{L}_1, \end{aligned} \quad (25)$$

where

$$\begin{aligned} L_1 &= \theta_1^2 - p_1 \phi_1 \\ L_2 &= -4\theta_2^3 + 5\theta_1 \theta_2^2 + (a\theta_1 + b\theta_2)\theta_1^2 + p_2 \phi_1 + p_3 \phi_2 \end{aligned} \quad (26)$$

are the PF operators¹⁶ and

$$\begin{aligned} p_1 &= (\theta_1 + \theta_2)(\theta_1 + 4\theta_2) \\ p_2 &= -a\theta_1^3 - (b + 5a)\theta_1^2 \theta_2 - (5b + 4a + 5)\theta_1 \theta_2^2 - (4b + 21)\theta_2^3 \\ p_3 &= 16(\theta_1 + 4\theta_2 - 1)(\theta_1 + 4\theta_2 - 2)(\theta_1 + 4\theta_2 - 3). \end{aligned} \quad (27)$$

Note that $L_k \Pi = 0 \implies \mathcal{L}_k \Pi = 0$, but not vice versa. There are six linearly independent solutions to the PF equations, corresponding to the six periods of the $\mathcal{M}_{(86,2)}$. To compute the periods we need the classical intersection numbers κ_{ijk} of $\mathcal{M}_{(86,2)}$. These can be read off from the PF operators as was explained in [37]. The procedure can be summarized as follows. The numbers are defined as

$$\kappa_{ijk} = \int J_i \wedge J_j \wedge J_k. \quad (28)$$

The J_k 's are (1,1)-forms on $\mathcal{M}_{(86,2)}$ that constitute a basis of the Kähler cone that is dual to the basis of the Mori cone, $l^{(k)}$. To find the intersection numbers one has to construct the ring of polynomials orthogonal to the ideal generated by $\lim_{\phi \rightarrow 0} L_k(\theta, \phi)$. The top elements of this ring encode the κ_{ijk} [37]. In our example, we obtain

$$\kappa_{122} = 4, \quad \kappa_{222} = 5 \quad (29)$$

and all other $\kappa_{ijk} = 0$. A non-trivial check of our results is the computation of the Euler characteristic of $\mathcal{M}_{(86,2)}$ [37]:

$$\chi(\mathcal{M}_{(86,2)}) = -\frac{1}{3} \sum_{i,j,k=1}^2 \left(\sum_{\beta=1}^2 l_{0\beta}^{(i)} l_{0\beta}^{(j)} l_{0\beta}^{(k)} + \sum_{\alpha=1}^7 l_{\alpha}^{(i)} l_{\alpha}^{(j)} l_{\alpha}^{(k)} \right) \kappa_{ijk} = 168, \quad (30)$$

which agrees with $\chi = 2(h^{1,1} - h^{2,1})$.

¹⁶The solutions to the PF equations are the same for all constants a and b .

3.2 Periods and monodromies

The fundamental period ω_0 is calculated using the Laurent polynomials of the manifold (15,16). We use the formula

$$\omega_0 = \frac{1}{(2\pi i)^5} \int_{\gamma} \frac{1}{f_1 f_2} \frac{dt_1}{t_1} \wedge \dots \wedge \frac{dt_5}{t_5} \quad (31)$$

where the contour γ is a product of five circles enclosing $t_i = 0$. We need to find the residue of the integrand, which is the constant term in $\frac{1}{f_1 f_2}$. This term can be found using the Mori generators. Using $f_i = 1 - g_i$ we get

$$\omega_0 = \frac{1}{(2\pi i)^5} \int_{\gamma} \sum_{m,n=0}^{\infty} g_1^m g_2^n \frac{dt_1}{t_1} \wedge \dots \wedge \frac{dt_5}{t_5}, \quad (32)$$

yielding

$$\omega_0 = \sum_{n_1, n_2} \frac{(n_1 + 4n_2)!(n_1 + n_2)!}{(n_1!)^2 (n_2!)^5} \phi_1^{n_1} \phi_2^{n_2}, \quad (33)$$

which is convergent near $\phi_i = 0$. Here ϕ_k are the complex structure moduli defined in equation (20). It is straight-forward to check that ω_0 solves the PF equations (26).

This period can also be obtained by the Frobenius method. Applying the PF operators to the ansatz

$$\omega_0 = \sum_{n_1, n_2} c(n_1, n_2) \phi_1^{n_1} \phi_2^{n_2}, \quad (34)$$

gives recursion relations for $c(n_1, n_2)$ that (33) satisfies. Since $\phi_i = 0$ is a regular singular point of the PF equations, this is the only power series solution near this point [38]. All other solutions contain logarithmic singularities; we obtain two periods with one logarithm, two periods with double logarithms and one period with triple logarithms. Let

$$\omega(\rho, \phi) = \sum_{n_1, n_2} c(n_1 + \rho_1, n_2 + \rho_2) \phi_1^{n_1 + \rho_1} \phi_2^{n_2 + \rho_2}. \quad (35)$$

The periods are then given by [37]

$$\begin{aligned} \omega_0 &= \omega|_{\rho=0} \\ \omega_1 &= D_1^{(1)} \omega \equiv \frac{1}{2\pi i} \partial_{\rho_1} \omega|_{\rho=0} \\ \omega_2 &= D_2^{(1)} \omega \equiv \frac{1}{2\pi i} \partial_{\rho_2} \omega|_{\rho=0} \\ \omega_3 &= D_1^{(2)} \omega \equiv \frac{1}{2(2\pi i)^2} \kappa_{1jk} \partial_{\rho_j} \partial_{\rho_k} \omega|_{\rho=0} \\ \omega_4 &= D_2^{(2)} \omega \equiv \frac{1}{2(2\pi i)^2} \kappa_{2jk} \partial_{\rho_j} \partial_{\rho_k} \omega|_{\rho=0} \\ \omega_5 &= D^{(3)} \omega \equiv \frac{1}{6(2\pi i)^3} \kappa_{ijk} \partial_{\rho_i} \partial_{\rho_j} \partial_{\rho_k} \omega|_{\rho=0}. \end{aligned} \quad (36)$$

The factors of $2\pi i$ are chosen in order to give integral monodromy matrices. Note that the intersection numbers (29), related to the leading parts of the PF operators when $\phi_i \rightarrow 0$, determine the linear combinations of $\partial_{\rho_k} \omega|_{\rho=0}$ that solve the equations.

Naturally, linear combinations of these periods yield other solutions. For our purpose of computing the monodromies of $\mathcal{M}_{(86,2)}$, it is interesting to find a basis of periods which has integral and symplectic monodromy matrices. Furthermore, we would like to find a basis of periods that is symplectic with a canonical symplectic metric, as described in appendix A.

It was discovered in [36, 37] that such a basis can be constructed, again using toric geometry. How to do this explicitly is clearly described in [39]. We start by choosing a basis of $H^{even}(\mathcal{M}_{(86,2)}, \mathbb{Q})$: $1, J_k, J_l^{(2)}, J^{(3)}$ are forms of degree 0,2,4 and 6 respectively that fulfill

$$\begin{aligned} (1, J^{(3)}) &= \int_{\mathcal{M}_{(86,2)}} 1 \wedge J^{(3)} = -1 \\ (J_k, J_j^{(2)}) &= \int_{\mathcal{M}_{(86,2)}} J_k \wedge J_j^{(2)} = \delta_{kj}. \end{aligned} \tag{37}$$

A canonical symplectic basis of even forms is then found by shifting $J_k \rightarrow J_k^{(1)} = J_k - \frac{c_2 \wedge J_k}{12}$, where c_2 is the second Chern class of the manifold [39]. This basis is symplectic with respect to the skew symmetric form

$$q_{\alpha\beta} = \langle \alpha, \beta \rangle = \int_{\mathcal{M}_{(86,2)}} \alpha \wedge (-1)^p \beta \wedge \text{Todd}(\mathcal{M}_{(86,2)}), \tag{38}$$

where α and β are $2q$ - and $2p$ -forms on $\mathcal{M}_{(86,2)}$, respectively. The Todd class for $\mathcal{M}_{(86,2)}$ is given by

$$\text{Todd}(\mathcal{M}_{(86,2)}) = 1 + c_1 + \frac{1}{12}(c_1^2 + c_2) + \frac{1}{24}c_1 c_2, \tag{39}$$

where c_i is the i^{th} Chern class of $\mathcal{M}_{(86,2)}$. Using $c_1 = 0$, it follows that the symplectic metric for the above basis of even forms is given by

$$q = \begin{pmatrix} 0 & 0 & 0 & 0 & 0 & 1 \\ 0 & 0 & 0 & 1 & 0 & 0 \\ 0 & 0 & 0 & 0 & 1 & 0 \\ 0 & -1 & 0 & 0 & 0 & 0 \\ 0 & 0 & -1 & 0 & 0 & 0 \\ -1 & 0 & 0 & 0 & 0 & 0 \end{pmatrix}. \tag{40}$$

The result of [39] is that the period basis

$$\begin{aligned}
\xi_0 &= \omega|_{\rho=0} \\
\xi_1 &= D_1^{(1)}\omega \\
\xi_2 &= D_2^{(1)}\omega \\
\xi_3 &= D_1^{(2)}\omega + \frac{1}{2\pi i} A_{1k} \partial_{\rho_k} \omega|_{\rho=0} \\
\xi_4 &= D_2^{(2)}\omega + \frac{1}{2\pi i} A_{2k} \partial_{\rho_k} \omega|_{\rho=0} \\
\xi_5 &= D^{(3)}\omega - \frac{1}{2\pi i} \frac{(c_2, J_k)}{12} \partial_{\rho_k} \omega|_{\rho=0}.
\end{aligned} \tag{41}$$

is integral and symplectic with respect to the same q . All that is needed to compute the new basis are the topological numbers A_{lk} and (c_2, J_k) , defined as [37]

$$\begin{aligned}
A_{lk} &= \frac{1}{2} \kappa_{llk} \bmod \mathbb{Z} \\
(c_2, J_k) &= \int_{\mathcal{M}_{(86,2)}} c_2 \wedge J_k = \frac{1}{2} \sum_{i,j} \sum_{\alpha} (l_{0,\alpha}^{(i)} l_{0,\alpha}^{(j)} - l_{\alpha}^{(i)} l_{\alpha}^{(j)}) \kappa_{ijk}.
\end{aligned} \tag{42}$$

Thus, for $\mathcal{M}_{(86,2)}$ we get

$$\begin{aligned}
A_{22} &= \frac{1}{2}, \text{ all other } A_{lk} = 0 \\
(c_2, J_1) &= 24 \text{ and } (c_2, J_2) = 50.
\end{aligned} \tag{43}$$

Carrying out the differentiations described in (41) we then obtain a basis of periods corresponding to a canonical basis of 3-cycles on $\mathcal{M}_{(86,2)}$.

In order to compute the monodromies around the two singular loci $\phi_1 = 0$ and $\phi_2 = 0$, we expand ξ near $\phi_i = 0$. We have

$$\begin{aligned}
\xi_0 &\sim 1 \\
\xi_1 &\sim \frac{1}{2\pi i} \ln \phi_1 \\
\xi_2 &\sim \frac{1}{2\pi i} \ln \phi_2 \\
\xi_3 &\sim -1 + \frac{2}{(2\pi i)^2} \ln^2 \phi_2 \\
\xi_4 &\sim -\frac{25}{12} + \frac{1}{2(2\pi i)} \ln \phi_2 + \frac{5}{2(2\pi i)^2} \ln^2 \phi_2 + \frac{4}{(2\pi i)^2} \ln \phi_1 \ln \phi_2 \\
\xi_5 &\sim \frac{21i\zeta(3)}{\pi^3} - \frac{25}{12(2\pi i)} \ln \phi_2 - \frac{1}{2\pi i} \ln \phi_1 - \frac{1}{6(2\pi i)^3} (5 \ln^3 \phi_2 + 12 \ln^2 \phi_2 \ln \phi_1).
\end{aligned} \tag{44}$$

The monodromies around $\phi_i = 0$ are easy to read off from the expansion of the periods around that point, equation (44). We find that the monodromy around $\phi_1 = 0$

is given by

$$t_2 = \begin{pmatrix} 1 & 0 & 0 & 0 & 0 & 0 \\ 1 & 1 & 0 & 0 & 0 & 0 \\ 0 & 0 & 1 & 0 & 0 & 0 \\ 0 & 0 & 0 & 1 & 0 & 0 \\ 0 & 0 & 4 & 0 & 1 & 0 \\ -2 & 0 & 0 & -1 & 0 & 1 \end{pmatrix} \quad (45)$$

and the monodromy around $\phi_2 = 0$ is

$$t_0 = \begin{pmatrix} 1 & 0 & 0 & 0 & 0 & 0 \\ 0 & 1 & 0 & 0 & 0 & 0 \\ 1 & 0 & 1 & 0 & 0 & 0 \\ 2 & 0 & 4 & 1 & 0 & 0 \\ 3 & 4 & 5 & 0 & 1 & 0 \\ -5 & -2 & -2 & 0 & -1 & 1 \end{pmatrix}. \quad (46)$$

We denote the monodromy matrices t_0 and t_2 in order to conform with the notation in [14]: see Appendix A.

4 Relating $\mathcal{M}_{(86,2)}$ to the mirror quintic

We now set out to find the locus in the moduli space of $\mathcal{M}_{(86,2)}$ that corresponds to the mirror quintic. Expanding the periods calculated in section 3 close to this locus will enable us to match periods between the two manifolds. In doing this, it is important to bear in mind that there are periods that vanish on the mirror quintic locus. To make the matching unique we must make use of the symplectic structure or, equivalently, of the monodromies around the locus.

Specifically, as we explain more thoroughly in section 5, one three-cycle¹⁷ A of $H_3(\mathcal{M}_{(86,2)}, \mathbb{Z})$ shrinks as we approach the mirror quintic. Its dual B becomes a three-chain as the two-spheres are blown up. The cycle B transforms nontrivially as the mirror quintic locus is encircled, and neither A nor B should intersect the cycles corresponding to the mirror quintic periods.

4.1 The mirror quintic locus

Approaching the mirror quintic locus means sending $\phi_1 \rightarrow 1$ and $\phi_2 \rightarrow 0$ in such a way that $\phi_2(1 - \phi_1)^{-4} \rightarrow 0$ while $\phi_1\phi_2(1 - \phi_1)^{-5}$ remains finite. To see this, we use the alternative description of $\mathcal{M}_{(86,2)}$ provided in [35], where this locus is determined. If

¹⁷See appendix A for notations.

we eliminate the variables t_1 and t_2 in favor of $t_1 t_2$ in the first equation of (15) using (16), and make the change of variables and coefficients

$$\begin{aligned} u_1 &= t_3, & u_2 &= t_4, & u_3 &= t_5, & u_4 &= t_1 t_2 \\ b_0 &= 1 - a_1 a_6, & b_1 &= -a_2, & b_2 &= -a_3, & b_3 &= -a_4, \\ b_4 &= -a_1 a_7, & b_5 &= -a_5 a_6, & b_6 &= -a_5 a_7 \end{aligned} \quad (47)$$

we obtain

$$b_0 + b_1 u_1 + b_2 u_2 + b_3 u_3 + b_4 u_4 + \frac{b_5}{u_1 u_2 u_3 u_4} + \frac{b_6}{u_1 u_2 u_3} = 0. \quad (48)$$

This is, up to notation, identical to equation (5.13) of [35]. The mirror quintic locus is $b_6 = 0$. Natural coordinates on moduli space are, from this point of view,

$$z_1 = \frac{b_1 b_2 b_3 b_6}{b_0^4} = \frac{\phi_2}{(1 - \phi_1)^4} \quad (49)$$

$$z_2 = -\frac{b_1 b_2 b_3 b_4 b_5}{b_0^5} = \frac{\phi_1 \phi_2}{(1 - \phi_1)^5}. \quad (50)$$

In the patch described by these coordinates the mirror quintic locus is $z_1 = 0$. We now turn to finding expressions for the periods valid close to this locus.

4.2 The fundamental period

Let us begin with the fundamental period for which it is possible to arrive at a very simple expression in terms of the variables (z_1, z_2) . The period is

$$\omega_0 = (1 - \phi_1) \sum_{n_1, n_2} \frac{(n_1 + 4n_2)!(n_1 + n_2)!}{(n_1!)^2 (n_2!)^5} \phi_1^{n_1} \phi_2^{n_2} = \quad (51)$$

$$= (1 - \phi_1) \sum_{n_2} \frac{(4n_2)!}{(n_2!)^4} {}_2F_1(4n_2 + 1, n_2 + 1, 1, \phi_1) \phi_2^{n_2}, \quad (52)$$

where the prefactor $(1 - \phi_1)$ has been chosen to make the period finite at the mirror quintic locus.¹⁸ We also introduced the hypergeometric function ${}_2F_1$.

By expressing ω_0 in the variables (z_1, z_2) we see explicitly that ω_0 reduces to the fundamental period of the mirror quintic as $z_1 \rightarrow 0$. Using the analytical continuation of ${}_2F_1$ given in 15.3.4 of [40] we have

$${}_2F_1(4n_2 + 1, n_2 + 1; 1; \phi_1) = (1 - \phi_1)^{-4n_2 - 1} {}_2F_1(4n_2 + 1, -n_2; 1; \frac{\phi_1}{\phi_1 - 1}) = \quad (53)$$

$$= (1 - \phi_1)^{-4n_2 - 1} \sum_{m_2=0}^{n_2} \frac{(4n_2 + m_2)! n_2!}{(4n_2)! (n_2 - m_2)! (m_2!)^2} \left(\frac{\phi_1}{1 - \phi_1} \right)^{m_2}. \quad (54)$$

¹⁸Note that it is always possible to rescale Ω , and hence the periods, by a holomorphic function of the moduli.

The expansion of the ${}_2F_1$ terminates since n_2 is a nonnegative integer. Therefore we can replace n_2 in favor of $m_1 = n_2 - m_2$ in the sum representing ω_0 , and thus obtain

$$\omega_0 = \sum_{m_1, m_2=0}^{\infty} \frac{(4m_1 + 5m_2)!}{((m_1 + m_2)!)^3 m_1! (m_2!)^2} z_1^{m_1} z_2^{m_2}. \quad (55)$$

The expansion (55) can be shown to be convergent for at least $|z_i| < 5^{-3}9^{-3}$. Taking $z_1 \rightarrow 0$ we recover the fundamental period of the mirror quintic [19] with $z_2 = (5\psi)^{-5}$:

$$\omega_0(z_1 = 0) = \sum_{m_2=0}^{\infty} \frac{(5m_2)!}{(m_2!)^5 (5\psi)^{5m_2}}. \quad (56)$$

4.3 The other periods

For the other periods it is difficult to find explicit expansions in the variables (z_1, z_2) , so we just study their values at the mirror quintic locus and their monodromies. The strategy is to analytically continue the ${}_2F_1$ from $\phi_1 \sim 0$ to $\phi_1 \sim 1$ using standard identities. To construct the five additional periods we need the following six derivatives

$$\partial_{\rho_1}\omega, \quad \partial_{\rho_2}\omega, \quad \partial_{\rho_2}\partial_{\rho_1}\omega, \quad \partial_{\rho_2}^2\omega, \quad \partial_{\rho_2}^2\partial_{\rho_1}\omega, \quad \partial_{\rho_2}^3\omega, \quad (57)$$

with

$$\omega(\rho, \phi) = (1 - \phi_1) \sum_{n_1, n_2} \frac{\Gamma(\tilde{n}_1 + 4\tilde{n}_2 + 1)\Gamma(\tilde{n}_1 + \tilde{n}_2 + 1)}{\Gamma^2(\tilde{n}_1 + 1)\Gamma^5(\tilde{n}_2 + 1)} \phi_1^{\tilde{n}_1} \phi_2^{\tilde{n}_2}. \quad (58)$$

For brevity we defined $\tilde{n}_i = n_i + \rho_i$. Note that $\omega(0, \phi) = \omega_0(\phi)$

Let us start with the three derivatives containing ∂_{ρ_1} . Differentiating once, evaluating at $\rho_1 = 0$ and using identity 15.3.10 of [40] we obtain

$$\partial_{\rho_1}\omega(\rho_2) = -(1 - \phi_1) \sum_{n_2=0} \frac{\Gamma^2(4\tilde{n}_2 + 1)}{\Gamma(5\tilde{n}_2 + 2)\Gamma^3(\tilde{n}_2 + 1)} {}_2F_1(4\tilde{n}_2 + 1, \tilde{n}_2 + 1; 5\tilde{n}_2 + 2; 1 - \phi_1)\phi_2^{\tilde{n}_2}. \quad (59)$$

The above equation is an expansion in $(1 - \phi_1)$ and ϕ_2 , both of which go to zero as we approach the mirror quintic. Because of the overall factor $(1 - \phi_1)$ there is no constant term, and differentiating with respect to ρ_2 will not change that. Thus all the derivatives $\partial_{\rho_1}\omega$, $\partial_{\rho_2}\partial_{\rho_1}\omega$ and $\partial_{\rho_2}^2\partial_{\rho_1}\omega$ vanish at the mirror quintic locus. These functions will, however, have monodromies around this locus. This is because each ∂_{ρ_2} that acts on $\phi_2^{\tilde{n}_2}$ produces a factor $\ln \phi_2 = 5 \ln(z_1) - 4 \ln(z_1 + z_2)$. It turns out that we need only the behavior of $\partial_{\rho_2}\partial_{\rho_1}\omega$. Carrying out the differentiation yields

$$\begin{aligned} \partial_{\rho_1}\omega &\sim 0, \\ \partial_{\rho_2}\partial_{\rho_1}\omega &\sim \ln \phi_2 \partial_{\rho_1}\omega. \end{aligned} \quad (60)$$

Here all terms off the mirror quintic locus that do not contain logarithms are ignored. For the three derivatives containing only ∂_{ρ_2} we can take $\rho_1 = 0$ and identify the n_1

sum as a hypergeometric function exactly as in (52). Then, using 15.3.6 of [40] it is straightforward to obtain.

$$\omega = \sum_{n_2} \frac{\Gamma(5\tilde{n}_2 + 1)}{\Gamma^5(\tilde{n}_2 + 1)} (z_1 + z_2)^{\tilde{n}_2} {}_2F_1(-4\tilde{n}_2, -\tilde{n}_2; -5\tilde{n}_2; 1 - \phi_1) - f(\rho_2) \partial_{\rho_1} \omega, \quad (61)$$

where

$$f(\rho_2) = \frac{\sin(\pi\rho_2) \sin(4\pi\rho_2)}{\pi \sin(5\pi\rho_2)}. \quad (62)$$

Differentiated with respect to ρ_2 and evaluated at $\phi_1 = 1$ and $z_1 = 0$, the first term of (61) yields exactly the four mirror quintic periods. As before, the second term and all its derivatives vanish at the mirror quintic locus, but transform nontrivially under transport around it. Taking the derivatives yields

$$\begin{aligned} \partial_{\rho_2} \omega &\sim \partial_{\rho_2} \omega^{MQ}, \\ \partial_{\rho_2}^2 \omega &\sim \partial_{\rho_2}^2 \omega^{MQ} - \frac{8}{5} \partial_{\rho_2} \partial_{\rho_1} \omega, \\ \partial_{\rho_2}^3 \omega &\sim \partial_{\rho_2}^3 \omega^{MQ} - \frac{12}{5} \partial_{\rho_2}^2 \partial_{\rho_1} \omega, \end{aligned} \quad (63)$$

where $\omega^{MQ} = \omega(\rho_1 = 0; z_1 = 0)$. Again, off the locus $z_1 = 0$, only terms that have monodromies around it are kept. Combining (60) and (63) we get for the basis ξ

$$\begin{aligned} \xi_0 &\sim \omega|_{\rho=0} \\ \xi_1 &\sim \frac{1}{2\pi i} \partial_{\rho_1} \omega \\ \xi_2 &\sim \frac{1}{2\pi i} \partial_{\rho_2} \omega^{MQ} \\ \xi_3 &\sim \frac{2}{(2\pi i)^2} \partial_{\rho_2}^2 \omega^{MQ} - 16 \frac{\ln z_1}{2\pi i} \xi_1 \\ \xi_4 &\sim \frac{5}{2(2\pi i)^2} \partial_{\rho_2}^2 \omega^{MQ} + \frac{1}{2(2\pi i)} \partial_{\rho_2} \omega^{MQ} \\ \xi_5 &\sim \frac{5}{6(2\pi i)^3} \partial_{\rho_2}^3 \omega^{MQ} - \frac{25}{6(2\pi i)} \partial_{\rho_2} \omega^{MQ}. \end{aligned} \quad (64)$$

The terms exhibiting monodromies around $z_1 = 0$ cancel in all basis periods except for ξ_3 . As the mirror quintic locus is encircled ξ_3 transforms as:

$$\xi_3 \rightarrow \xi_3 - 16\xi_1. \quad (65)$$

We will motivate the appearance of the number 16 in section 5.

4.4 The proper basis

From the analysis in the previous subsection it is clear that the periods corresponding to the shrinking three-cycles A and its dual B are ξ_1 and ξ_3 , i.e.,

$$\xi_1 = \oint_A \Omega, \quad \xi_3 = \oint_B \Omega. \quad (66)$$

The other four ξ_i correspond to integrals over the cycles that remain in the mirror quintic manifold. By using their asymptotic forms as $z_2 \rightarrow 0$, it is straightforward to relate them to the basis for the mirror quintic periods used in [14]:

$$\Pi = m\xi = \begin{pmatrix} 0 & 0 & 0 & 0 & 0 & 1 \\ 0 & 0 & -5 & 0 & -1 & 0 \\ 0 & 0 & 1 & 0 & 0 & 0 \\ 1 & 0 & 0 & 0 & 0 & 0 \\ 0 & 1 & 0 & 0 & 0 & 0 \\ 0 & 0 & 0 & 1 & 0 & 0 \end{pmatrix} \xi. \quad (67)$$

Here Π_1, \dots, Π_4 correspond to those of [14], meaning that Π_5 and Π_6 are the new periods. In the new basis the symplectic metric becomes

$$Q = mqm^T = \begin{pmatrix} 0 & 0 & 0 & -1 & 0 & 0 \\ 0 & 0 & 1 & 0 & 0 & 0 \\ 0 & -1 & 0 & 0 & 0 & 0 \\ 1 & 0 & 0 & 0 & 0 & 0 \\ 0 & 0 & 0 & 0 & 0 & 1 \\ 0 & 0 & 0 & 0 & -1 & 0 \end{pmatrix}, \quad (68)$$

and the monodromy matrices of section 3 become

$$T_0 = mt_0m^{-1} = \begin{pmatrix} 1 & 1 & 3 & -5 & -2 & 0 \\ 0 & 1 & -5 & -8 & -4 & 0 \\ 0 & 0 & 1 & 1 & 0 & 0 \\ 0 & 0 & 0 & 1 & 0 & 0 \\ 0 & 0 & 0 & 0 & 1 & 0 \\ 0 & 0 & 4 & 2 & 0 & 1 \end{pmatrix} \quad (69)$$

and

$$T_2 = mt_2m^{-1} = \begin{pmatrix} 1 & 0 & 0 & -2 & 0 & -1 \\ 0 & 1 & -4 & 0 & 0 & 0 \\ 0 & 0 & 1 & 0 & 0 & 0 \\ 0 & 0 & 0 & 1 & 0 & 0 \\ 0 & 0 & 0 & 1 & 1 & 0 \\ 0 & 0 & 0 & 0 & 0 & 1 \end{pmatrix}. \quad (70)$$

The upper four by four corner of T_0 precisely coincides with the large complex structure monodromy for the mirror quintic as given in [14].

Two additional monodromies are the conifold monodromies: one around the mirror quintic conifold locus, and the other around the mirror quintic locus itself. In the Π -basis, these are

$$T_1 = \begin{pmatrix} 1 & 0 & 0 & 0 & 0 & 0 \\ 0 & 1 & 0 & 0 & 0 & 0 \\ 0 & 0 & 1 & 0 & 0 & 0 \\ 1 & 0 & 0 & 1 & 0 & 0 \\ 0 & 0 & 0 & 0 & 1 & 0 \\ 0 & 0 & 0 & 0 & 0 & 1 \end{pmatrix} \quad (71)$$

and

$$T_{MQ} = \begin{pmatrix} 1 & 0 & 0 & 0 & 0 & 0 \\ 0 & 1 & 0 & 0 & 0 & 0 \\ 0 & 0 & 1 & 0 & 0 & 0 \\ 0 & 0 & 0 & 1 & 0 & 0 \\ 0 & 0 & 0 & 0 & 1 & 0 \\ 0 & 0 & 0 & 0 & -16 & 1 \end{pmatrix}. \quad (72)$$

This concludes our description of the geometry of $\mathcal{M}_{(86,2)}$ and how it reduces to the mirror quintic.

5 Geometric transitions in flux compactifications

We want to take a closer look at geometric transitions in the cases where fluxes through the relevant cycles are involved. Some of these cases have been well-studied in the literature; others are less understood.

5.1 Geometric transition: absence of fluxes

Let us first describe in some detail what happens to the homology of the manifold in the case where we make a geometric transition from $\mathcal{M}_{(86,2)}$ to the mirror quintic $\mathcal{M}_{(101,1)}$ *without* any fluxes on the relevant cycles. This discussion is exactly the mirror of the more familiar story for the ordinary quintic [17, 35].

In the transition, one three-homology class disappears. However, to obtain the right Hodge numbers we actually need sixteen three-spheres to shrink. We will denote these three-spheres by \mathcal{A}_i , $1 \leq i \leq 16$. Since they are all in the same homology class, there are fifteen homology relations of the form

$$\mathcal{A}_1 - \mathcal{A}_2 = \delta\mathcal{D}_1 \quad \cdots \quad \mathcal{A}_{15} - \mathcal{A}_{16} = \delta\mathcal{D}_{15} \quad (73)$$

where the \mathcal{D}_i are four-chains with boundary. For symmetry reasons it is useful to include a sixteenth four-chain $\mathcal{D}_{16} = -\sum_{i=1}^{15} \mathcal{D}_i$ in the discussion, so that $\mathcal{A}_{16} - \mathcal{A}_1 = \delta\mathcal{D}_{16}$. Finally, we have also to consider a cycle \mathcal{B} in the homology class dual to the class A that the $\{\mathcal{A}_i\}$'s belong to. This cycle will intersect the shrinking ones with intersection number 1:

$$\mathcal{A}_i \cap \mathcal{B} = 1. \quad (74)$$

We have drawn the different cycles and chains in figure 2a.

In the transition (see figure 2b) all sixteen \mathcal{A}_i shrink to points, and then get blown up into two-spheres a_i . These are not homologically independent but form the boundary of \mathcal{B} :

$$\delta\mathcal{B} = \sum a_i \quad (75)$$

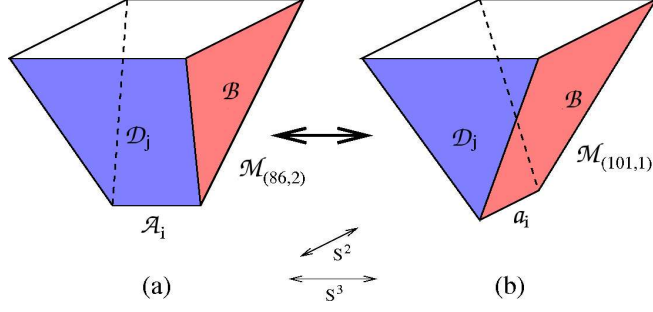


Figure 2: The familiar picture of a geometric transition on a single node: the S^3 denoted by \mathcal{A}_i shrinks, and the S^2 denoted by a_i blows up. In our example, sixteen of those transitions occur simultaneously.

Conversely, the \mathcal{D}_i lose their boundaries and now become closed:

$$\delta \mathcal{D}_i = 0 \quad 1 \leq i \leq 16 \quad (76)$$

Of course, we still have that $\sum \mathcal{D}_i = 0$, so the sixteen cycles \mathcal{D}_i actually represent fifteen homology classes. The relations (73) now turn into intersection relations:

$$\mathcal{D}_1 \cap a_1 = 1, \quad \mathcal{D}_1 \cap a_2 = -1 \quad (77)$$

$$\mathcal{D}_2 \cap a_2 = 1, \quad \dots \quad (78)$$

and so on.

Summarizing, we see that we lose two dual three-homology classes A and B , corresponding to one complex structure modulus, and we gain fifteen two-homology classes a_i and fifteen four-homology classes \mathcal{D}_i , corresponding to fifteen Kähler moduli.

Finally, the Picard–Lefschetz formula (see for example [41]) says that

$$\mathcal{B} \rightarrow \mathcal{B} + \sum_{i=1}^{16} (\mathcal{B} \cap \mathcal{A}^i) \mathcal{A}^i = \mathcal{B} - \sum_{i=1}^{16} \mathcal{A}^i \quad (79)$$

under transport around the transition locus in moduli space, where the cycles \mathcal{A}^i shrink. Thus, the homology classes transform as $B \rightarrow B - 16A$. This explains the appearance of the number 16 in (65).

5.2 Geometric Transition: presence of fluxes

We now discuss what happens in a geometric transition if we turn on fluxes through the relevant cycles \mathcal{A}_i and \mathcal{B} . There are three different cases; in some it is clear what happens, in others it is less so.

i. Only flux through the \mathcal{A}_i -cycles.

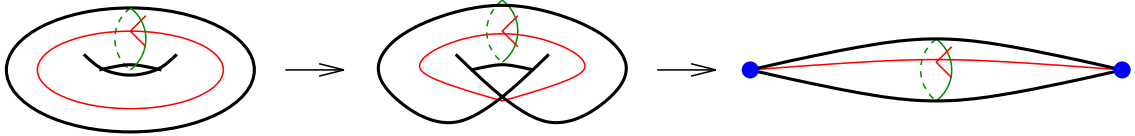


Figure 3: *The case with flux through the shrinking \mathcal{A}_i -cycles. The green line is the cycle, the red line is the magnetic flux. As the \mathcal{A}_i -cycles shrink the flux line is cut open. When the two-spheres blow up, five-branes (blue dots) appear, charging the flux. (Note that a zero-dimensional boundary automatically consists of two points; in the conifold case every conifold will of course give rise to only one brane.)*

This case has been well-studied in the literature [42, 43]. After the geometric transition, we find branes wrapped on the cycles a_i . If we start with a single unit of NS-flux through \mathcal{A}_i , then after the transition we will find a single NS5-brane wrapping each of the a_i and stretching throughout space-time. These branes are now the sources for the magnetic flux of the three-form field strength. In a lower-dimensional analogue, we can think of the magnetic field lines as having been “cut open” – see figure 3 for a cartoon. Similarly, if we start with a single unit of RR-flux through \mathcal{A}_i , we end up with D5-branes on a_i .

We encounter a complication when we want to compute the mirror quintic potential for this case, however. When we come back to the mirror quintic side, in the presence of the five-branes, the closed string moduli are no longer the only moduli of the system. In particular, as was explained in [44, 45, 46, 47] (see [48] for a good review), there will be some new open string moduli t_α describing the positions of the branes in A . These moduli appear in a new period, which is the holomorphic volume of the chain \mathcal{B} with boundary $\sum a_i$:

$$\Pi_{\mathcal{B}}(t_\alpha, z_2) = \int_{\mathcal{B}} \Omega, \quad (80)$$

where the z_2 is the closed string modulus. Just like the periods of the closed cycles, this period contributes to the four-dimensional superpotential:

$$W_{\mathcal{B}}(t_\alpha, z_2) = N \Pi_{\mathcal{B}}, \quad (81)$$

where N is the number of five-branes.

Because of this complication, in our explicit calculations we consider the case where we get no five-branes after the transition. It would of course be very interesting to extend our calculations to the full case including five-branes.

An interesting possibility of the appearance of five-branes is that we can now construct domain walls between configurations with and without five-branes. We will briefly discuss this issue in subsection 5.4.

ii. Only flux through the \mathcal{B} -cycle.

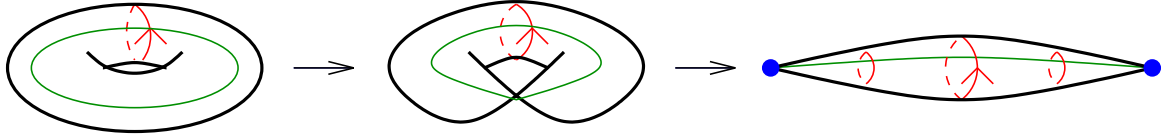


Figure 4: *The case with flux through the tearing \mathcal{B} -cycle. The green line is the cycle, the red line is the flux. After the geometric transition the flux goes through a chain. This flux is possibly charged by one-instantons (blue dots).*

Next, we discuss the case where we only have flux through the dual cycle \mathcal{B} of the vanishing cycle, but no flux through the vanishing cycle itself. In this case, since $\int F_{(3)} \wedge H_{(3)} = 0$, the flux does not represent any D3-brane charge, so there is no conservation condition that forces the nucleation of e.g. D3-branes.

Furthermore, as we show in the next subsection, the contribution to the scalar potential from this kind of flux vanishes at the transition locus. Therefore, we expect no problems when going through the geometric transition.¹⁹

It is possible that the flux remains on the other side of the transition, sourced by electrically charged D1-instantons or F1-instantons on the blown up two-spheres. (See [50] for a recent discussion on D1-instantons in geometric transitions.) A cartoon of this scenario is given in figure 4. When there is no flux through the \mathcal{A}_i -cycles (that is, no D5-branes are present after the transition), these instantons do not contribute to the (super)potential on the resolved side.

For these reasons, this case is under much more control than the case (i), and it is the one which we will study in our example in section 6.

iii. Flux through the \mathcal{A}_i - and \mathcal{B} -cycles.

This is the most complicated scenario. We will not make any rigorous claims about what happens, but let us discuss some possible outcomes.

First of all, as we mentioned in (i), it is natural to assume that the \mathcal{A}_i -fluxes turn into five-branes around a_i . To picture the fate of the fluxes through \mathcal{B} , one suggestion comes from the well-known Klebanov–Strassler setup [51]. In this case, one studies the deformed conifold, which is a non-compact Calabi–Yau manifold with a compact three-cycle A that shrinks, and a dual non-compact three-cycle B . There are N units of RR-flux through the A -cycle, and M units of NS-flux through the B -cycle. The total D3 charge coming from the three-flux background ($\int F_{(3)} \wedge H_{(3)}$) and the presence of D3-branes and orientifold three-planes must be conserved and therefore be equal on the two sides of the transition. In particular, the above mentioned fluxes piercing the A - and B -cycles give a contribution $K = MN$ to the total charge.

After the transition, the deformed conifold becomes a resolved conifold, which has a new two-cycle a instead of the three-cycle A . One now finds N D5-branes on a , as

¹⁹Indeed, it has been argued [49] that, after the geometric transition, no fluxes or branes whatsoever remain. We thank S. Kachru for useful discussions on this case and on the case (iii).

could be expected from the case (i). Moreover, the contribution to the total charge, previously coming from the fluxes, now comes from $K = MN$ new D3-branes that fill the perpendicular space-time.

In our compact case, the sixteen nodes locally look like conifolds, so a first possibility is that the same thing happens: if we have N units of RR-flux through the \mathcal{A}_i and M units of NS-flux through \mathcal{B} , we will find N D5-branes on the a_i and $K = MN$ space-time filling D3-branes after the transition, so that the charge conservation condition is satisfied.

With case (ii) in mind one might instead expect that the fluxes remain, charged by both five-branes and one-instantons. This situation could either be stable, or decay into the D3-brane configuration described above.

We may also wonder what happens to fluxes that do not contribute to the total D3-brane charge. For example, we could have some RR-flux through \mathcal{A}_i , and some RR-flux through \mathcal{B} as well. As in case (i) the flux through \mathcal{A}_i will result in five-branes. However, no D3-branes will be generated, and as in (ii), we might conjecture that after the transition, either the fluxes through \mathcal{B} completely disappear or remain charged by one-instantons. It would be interesting to investigate these possibilities further.

Finally, we note that also in this case, as in (i), there will be new open-string moduli in the theory after the transition. For this reason, we will not treat this case in our explicit calculations below.

5.3 The scalar potential

Fluxes piercing the cycles of $\mathcal{M}_{(86,2)}$ induce a potential for the two complex structure moduli. It is important to know the properties of this potential to fully understand the geometric transition between $\mathcal{M}_{(86,2)}$ and the mirror quintic. In particular, we need to study the behavior of the potential as we approach the transition locus $z_1 = 0$ in the complex structure moduli space of $\mathcal{M}_{(86,2)}$.

We expand the periods near $z_1 = 0$ and, with a convenient notation, obtain the leading order behavior

$$\Pi(z_1, z_2) \sim \begin{pmatrix} \pi_1(z_2) + \mathcal{O}(z_1) \\ \pi_2(z_2) + \mathcal{O}(z_1) \\ \pi_3(z_2) + \mathcal{O}(z_1) \\ \pi_4(z_2) + \mathcal{O}(z_1) \\ z_1 \pi_5(z_2) + \mathcal{O}(z_1^2) \\ \pi_6(z_2) - \frac{16}{2\pi i} z_1 \ln(z_1) \pi_5(z_2) + \mathcal{O}(z_1^2 \ln(z_1)) \end{pmatrix}. \quad (82)$$

The no-scale potential²⁰ is given by

$$V(z, \tau) = e^K (g^{i\bar{i}} D_i W D_{\bar{i}} \bar{W} + g^{\tau\bar{\tau}} D_{\tau} W D_{\bar{\tau}} \bar{W}) \quad (83)$$

²⁰See Appendix A for notations.

where W is the superpotential and K is the Kähler potential.

Keeping only the leading terms for $z_1 \rightarrow 0$, we find that the potential is given by $V = V_1 + V_2$, where:

$$V_1(z_1, z_2) \equiv e^K (g^{1\bar{1}} D_1 W D_{\bar{1}} \bar{W})|_{z_1 \rightarrow 0} \quad (84)$$

$$V_2(z_2) \equiv e^K \left(g^{2\bar{2}} D_2 W D_{\bar{2}} \bar{W} + g^{\tau\bar{\tau}} D_\tau W D_{\bar{\tau}} \bar{W} \right)|_{z_1 \rightarrow 0}. \quad (85)$$

Note that terms containing $g^{1\bar{2}}$ and $g^{\bar{1}2}$ are subleading. This potential has different properties, depending on the presence of fluxes piercing different cycles. In particular:

- if there is flux F_6, H_6 through the shrinking cycle, the potential has an infinite spike at the conifold locus. At leading order we obtain:

$$V_1 \sim \ln |z_1| \frac{1}{|\tau - \bar{\tau}|} |F_6 - \tau H_6|^2 |\pi_5(z_2)|^2. \quad (86)$$

- if there is no F_6 nor H_6 , but flux F_5, H_5 through B we obtain:

$$V_1 \sim \frac{1}{\ln |z_1|} \frac{1}{|\tau - \bar{\tau}|} |F_5 - \tau H_5|^2 |\pi_5(z_2)|^2 \quad (87)$$

and this part of the potential goes to zero at the conifold locus.²¹ This is a general behavior for all compactifications on Calabi–Yau threefolds which have conifold singularities, as noted in [14].

This flux dependence of the potential fits well with the expected behavior within a geometric transition with different fluxes. V_2 is the part of the potential that is created by fluxes wrapping the mirror quintic cycles. Thus it gives the “ordinary” flux potential for the complex structure modulus z_2 on the mirror quintic. V_1 captures the dependence of the flux through the shrinking and torn cycles A and B , giving different scenarios.

Let us start with the case having flux through the shrinking cycle A in $\mathcal{M}_{(86,2)}$, but not through the torn one B . As discussed in section 5.2, there will be contributions from five-branes to the potential for the mirror quintic when we go through the conifold transition. The behavior of the $\mathcal{M}_{(86,2)}$ potential agrees with this. Indeed, if F_6 or H_6 are non-zero there are non-vanishing terms left in V_1 , even after setting $z_1 = 0$. We even find an infinite spike. When moving away from the conifold point in the Kähler moduli space of the mirror quintic, it is plausible that the new terms become finite and match the terms coming from a five-brane contribution. As a side remark, it is tempting to think of the open string moduli of the branes as a remnant of the complex structure modulus that one loses.

On the other hand, if there is zero flux through the A cycle, but a non-zero one through the B cycle, the terms that remain as $z_1 \rightarrow 0$ in the $\mathcal{M}_{(86,2)}$ potential match

²¹If we minimize the potential with respect to the axio-dilaton τ at the conifold locus, we find the result of [14], i.e. $V_1 \sim \frac{1}{\sqrt{K_{z_1 \bar{z}_1}}}$.

the terms on the mirror quintic side. Assuming that we do not generate other terms moving in the Kähler moduli space of the mirror quintic, there is no need for extra branes after the transition.

Finally, when we have fluxes through both A and B , or only through A , we find terms in V_1 which remain finite in the limit $z_1 \rightarrow 0$. It is natural to assume that they will also be present after the transition, and will vary in a continuous manner as a function of the Kähler moduli of the mirror quintic. As mentioned in the previous subsection, it is not clear what the physical description of the system after the transition should be, but it would be an interesting test of any proposal for such a description to see if it reproduces these terms in the appropriate limit.

5.4 Flux on the vanishing cycle: domain walls

If there is a flux on the vanishing three-cycle, our calculations show that the potential blows up as we approach the mirror quintic locus (see equation (86)). That is, as the three-spheres contract, the potential grows. Going through the geometric transition, the vanishing three-spheres are replaced by vanishing two-spheres, and the flux is replaced by five-branes wrapping the two-cycles, as discussed above.

It is natural to expect that there is a corresponding growth in the potential if we approach the locus from the side of the mirror quintic, this time due to the vanishing two-cycles wrapped by five-branes. We therefore conclude that if all effects from closed and open string moduli are included, there will be a contribution to the potential on the mirror quintic side that is inversely proportional²² to the volume of the appropriate two-cycles. The picture we have in mind is that of a spike in the potential, separating the phase of the mirror quintic with five-branes and the phase of the $\mathcal{M}_{(86,2)}$ with fluxes.

It is interesting to speculate on the possibility of actually penetrating through the spike separating the two phases. Classically this would be possible if the spike is cut off at a finite height by effects due to stringy and non-perturbative physics. If this is indeed what happens, there is a possibility of obtaining domain walls separating regions with and without wrapped five-branes. (See [50] for a recent discussion on transitions between phases with and without branes.)

Let us start with the mirror quintic without five-branes, and then move through the Kähler moduli space toward the appropriate transition locus that takes us to the $\mathcal{M}_{(86,2)}$. Without five-branes there is no prominent barrier that prevents us from doing this. We then encircle an appropriate locus resulting in a monodromy that generates flux through the vanishing cycle. The monodromy obtained in (70) is an example of such a monodromy, as we will see in more detail in the next section. When we then go back toward the mirror quintic locus, we find a high barrier that we need to cross. In contrast to the situation we started with, we now have five-branes extending through space-time and wrapping internal two-cycles.

²²It is clear that the potential should grow. For arguments as to why it should grow with the inverse volume, see [52].

We can use this idea to construct domain walls. Let us take one space-time direction, say the x -direction, and put our system in the phase without five-branes in the region $x \rightarrow -\infty$, and in the phase with five-branes in the region $x \rightarrow \infty$. In between these regions, the system will change in a continuous manner, which will be exactly described by our path through moduli space. That is, macroscopically, we will see a domain wall with five-branes ending on one of its sides. Microscopically, we have a barrier whose profile is described by the potential as a function of the continuous path through moduli space.

We can also speculate on the possibility of tunneling from one side to the other. This would be relevant for tunneling between minima connected by paths in moduli space going through the geometric transition. It is interesting to note that a rough estimate of the tunneling amplitude gives the result

$$e^{-\int \sqrt{g}V(\phi)} = e^{-\int_0^{\phi_i} \sqrt{\ln \phi} \ln \phi} \sim \text{finite} \quad (88)$$

even without a regularization of the singular point $\phi = 0$. Assuming that there is no dramatic difference on the Kähler side of the spike we see that there is good reason to expect a finite tunneling amplitude.

In the next section we return to the more solid ground of the case with no flux on the vanishing cycle.

6 Infinite series of minima

As discussed in the introduction, monodromy transformations create continuous paths between minima of the flux-induced potential in Calabi–Yau compactifications [14]. The transformations take us between minima corresponding to different fluxes. Here we investigate the length of such series of minima. We would like to understand if infinite series of continuously connected minima are a topographic feature of our model of the string theory landscape.²³

In [14], it was found that infinite series of minima do exist in compactifications on the mirror quintic, but it was unclear if these series can be connected by monodromy transformations. We now use geometric transitions to reach the moduli space of $\mathcal{M}_{(86,2)}$. In this way, we obtain new monodromies, creating new continuous paths between minima. As we now explain, these new transformations yield infinite series of continuously connected minima.

²³As discussed in the introduction, we are only studying minima of the potential created by fluxes. These will be *vacua* in the string theory landscape if the Kähler moduli are stabilized and the back-reaction of the fluxes on the manifold can be neglected.

6.1 General considerations

In order to find a series of minima we are interested in monodromies T such that the vector of flux quanta²⁴ transforms as

$$F_n = F_0 T^n = F_0 + n F_L, \quad (89)$$

which is achieved using a monodromy matrix of the form

$$T = \mathbf{1} + \Theta, \quad (90)$$

where $\Theta^2 = 0$ and $F_0 \Theta = F_L$. For simplicity we will impose

$$H_n = H_L, \quad (91)$$

with $H_L \Theta = 0$. If there is a minimum to the potential induced by the flux vectors F_L and H_L , it follows that a series of fluxes F_n and H_L provide us with an infinite series of minima that asymptotes to the minimum given by F_L and H_L [14].

As is well-known, the total charge on a compact manifold \mathcal{M} must be zero. The three-form-fluxes, $F_{(3)}$ and $H_{(3)}$, yield a three-brane charge, that must be compensated by charges from three-branes and orientifold planes [53]:

$$\int_{\mathcal{M}} F_{(3)} \wedge H_{(3)} + Q_{D3} - Q_{O3} = 0. \quad (92)$$

If the fluxes are changed in a way that alters $\int_{\mathcal{M}} F_{(3)} \wedge H_{(3)} = F \cdot Q \cdot H \equiv F \wedge H$, the number of three-branes and orientifold planes must adjust in order to keep this tadpole condition satisfied. This requires the use of new physics, e.g. the nucleation of branes.

On the other hand, if we demand that $F_L \wedge H_L = 0$, the series of minima will have a constant $F_n \wedge H_n$ leaving the tadpole condition unchanged. Thus, in this case, there is no need to nucleate branes. This was the situation studied in [14] and is what we will focus on here.

Let us study the properties of the monodromy matrix $T = \mathbf{1} + \Theta$. Assume that the rank of Θ is r . We can then write

$$\Theta = \sum_{i=1}^r \Theta^{(i)} \quad (93)$$

where

$$\Theta_{kl}^{(i)} = b_k^{(i)} a_l^{(i)}, \quad (94)$$

with $\{b^{(i)}\}$ and $\{a^{(i)}\}$ each being a set of r linearly independent vectors. It follows from $\Theta^2 = 0$ that

$$b^{(i)} \cdot a^{(j)} = 0 \quad \forall i, j = 1..r, \quad (95)$$

²⁴Our notation is explained in appendix A.

and we see from

$$F_0\Theta = \sum_{i=1}^r (F_0 \cdot b^{(i)}) a^{(i)} = F_L, \quad (96)$$

that F_L necessarily lies in the r -dimensional subspace spanned by $\{a^{(i)}\}$. If the dimensionality of the flux space is $2d$, it is obvious that we must have $r \leq d$.

The difficult part is now to find a monodromy $T = \mathbf{1} + \Theta$ such that the space $\{a^{(i)}\}$ actually does contain flux vectors giving rise to a minimum. In [14], for the case of the mirror quintic, we were able to find transformations with the right property but unable to show that they were monodromies. Let us now examine whether the extension of the moduli space to the $\mathcal{M}_{(86,2)}$ changes the situation.

6.2 Series of minima in mirror quintic compactifications

In section 4 we generalized the action of the two independent monodromies on periods for the mirror quintic to periods of the $\mathcal{M}_{(86,2)}$. We also found two new monodromies. Interestingly, our new monodromies are precisely of the form discussed in the previous subsection. For $T_2 = \mathbf{1} + \Theta_2$ we find the rank three matrix

$$\Theta_2 = \begin{pmatrix} 0 & 0 & 0 & -2 & 0 & -1 \\ 0 & 0 & -4 & 0 & 0 & 0 \\ 0 & 0 & 0 & 0 & 0 & 0 \\ 0 & 0 & 0 & 0 & 0 & 0 \\ 0 & 0 & 0 & 1 & 0 & 0 \\ 0 & 0 & 0 & 0 & 0 & 0 \end{pmatrix}, \quad (97)$$

consistent with

$$\begin{aligned} a^{(1)} &= (0, 0, 0, -2, 0, -1) & b^{(1)} &= (1, 0, 0, 0, 0, 0) \\ a^{(2)} &= (0, 0, -4, 0, 0, 0) & b^{(2)} &= (0, 1, 0, 0, 0, 0) \\ a^{(3)} &= (0, 0, 1, 0, 0, 0) & b^{(3)} &= (0, 0, 0, 1, 0, 0). \end{aligned} \quad (98)$$

In addition to the conditions (95) it is easy to check that also

$$a^{(i)} \wedge a^{(j)} = 0 \quad \forall i, j = 0..3 \quad (99)$$

$$b^{(i)} \wedge b^{(j)} = 0 \quad \forall i, j = 0..3. \quad (100)$$

The first of these statements makes sure that $F_L \wedge H_L = 0$ is automatic if F_L and H_L lie in the space spanned by the $a^{(i)}$.

We now need to find $F_L \in \{a^{(i)}\}$ and $H_L \in \{a^{(i)}\}$ such that when we restrict the flux vectors to the four dimensional mirror quintic flux space, there is a minimum of the potential. If we can achieve this we have found an infinite series of continuously connected minima, even though we have to make geometric transitions to $\mathcal{M}_{(86,2)}$ and back again when we pass from one minimum to the next.

We have not been able to find any minima using the $T_2 = \mathbf{1} + \Theta_2$ above. However, by the use of the monodromy matrices T_0 and T_1 , we can rotate the space spanned

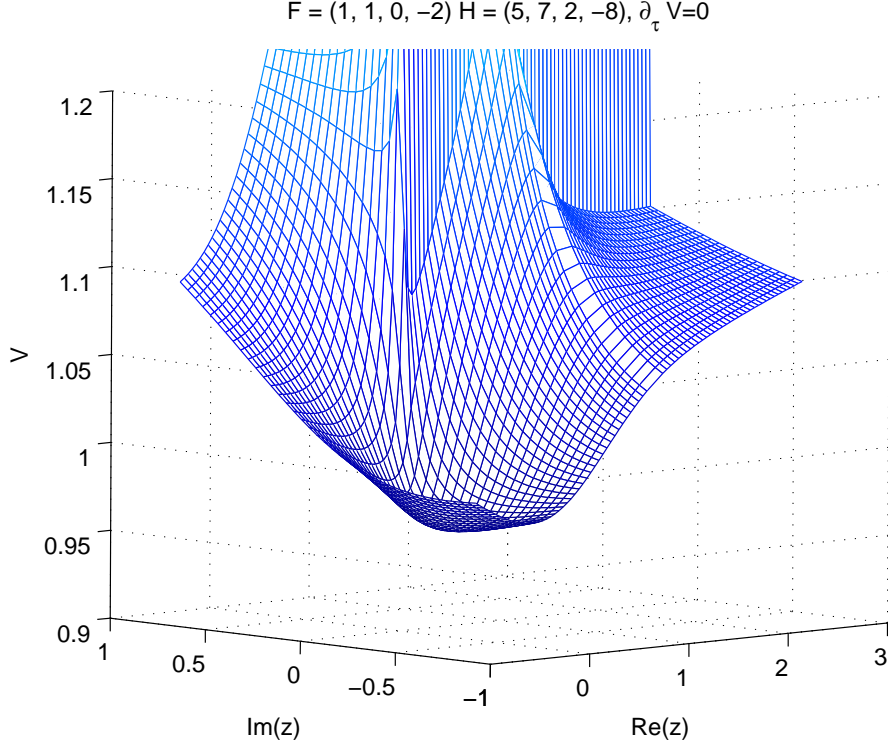


Figure 5: *The flux-induced potential V plotted on the complex structure moduli space of the mirror quintic. The plot shows $V(z, \tau(z))$, which is already minimized with respect to the axio-dilaton τ . The complex structure modulus of the mirror quintic is $z = 5^{-5}z_2$, where z_2 is a complex structure modulus of $\mathcal{M}_{(86,2)}$. The flux vectors are examples of fluxes obtained by applying the monodromy $\tilde{T} = 1 + \tilde{\Theta}$ many times. This minimum proves that there exist infinite series of continuously connected minima.*

by $\{a^{(i)}\}$ in such a way that minima are possible to find. A particular example is provided through the conjugation

$$\tilde{\Theta} = T_2^{-1}T_1T_0T_1\Theta_2T_1^{-1}T_0^{-1}T_1^{-1}T_2 \quad (101)$$

$$(102)$$

$$= \begin{pmatrix} 2 & 10 & -4 & 4 & 20 & 6 \\ 0 & 4 & -4 & 4 & 8 & 4 \\ -4 & -2 & -4 & 10 & -4 & 3 \\ 2 & 4 & 0 & -2 & 8 & 1 \\ 1 & -3 & 4 & -6 & -6 & -4 \\ -8 & -4 & -8 & 20 & -8 & 6 \end{pmatrix} \quad (103)$$

It is straightforward to see that any F_L obtained from $\tilde{\Theta}$ must be of the form

$$F_L = \left(f_1, f_2, f_3, -3f_1 + f_2, 2f_2, \frac{-f_1+f_2-f_3}{2} \right), \quad (104)$$

and correspondingly for H_L . We can choose the initial flux as

$$F_0 = \left(-\frac{f_1}{2} + \frac{f_2}{3} + \frac{f_3}{3}, f_1 - \frac{f_2}{2} - \frac{3f_3}{4}, -\frac{f_1}{2} + \frac{f_2}{6} + \frac{f_3}{6}, 0, 0, 0 \right), \quad (105)$$

to obtain such a flux vector.

Our numerical investigations show that it is easy to find minima with flux vectors of the form (104). However, if we want to make sure that we can easily go through the geometric transition, there are further restrictions on the flux. The flux that pierces the shrinking cycle induces a potential barrier at the transition locus, as discussed in subsection 5.3. This corresponds to the generation of five-branes in the geometric transition. Thus, in order to have a potential that is under full control, the flux through the shrinking cycle must vanish. This implies that the last component of the flux vector, that is $-f_1 + f_2 - f_3$, is zero, and correspondingly for H_L .

Even with this restriction it is possible to find minima. One example is shown in figure 5. The potential in the figure was computed numerically, as described in appendix A. The flux configurations, $F_L = (1, 1, 0, -2)$ and $H_L = (5, 7, 2, -8)$, correspond to limiting fluxes obtained after many transformations with $\tilde{T} = \mathbf{1} + \Theta$. Since acting with \tilde{T} on these fluxes produces a new minimum, we conclude that infinite series of continuously connected minima do exist for our model of the string theory landscape.

7 Conclusions

This work was originally triggered by a question left open in a previous investigation on the topography of the string landscape [14]. There, the focus was on determining the existence of families of string vacua (possibly metastable) connected through continuous paths in the landscape. The results of that work indicated that the landscape consists of a set of separate “islands”, such that minima on the same island are connected continuously, but another island could be reached only through disconnected “jumps”. What we have shown in the present paper is how to enlarge the kind of transformations acting on the periods and fluxes of a particular theory, and possibly continuously connect islands that were not connected within the original setting.

The presence of these new transformations follows from the interconnections among different models represented by geometric transitions, and represents a natural characteristic of the landscape. In particular, it leads to the discovery of *infinite* series of continuously connected minima for type IIB string theory in the mirror quintic. An example of these results can be found in section 6. As we have discussed, we expect effects due in particular to the stabilization of the Kähler moduli, which we do not investigate, that will shorten these series and make them finite. Nevertheless, the existence of long series of many closely spaced vacua is an interesting topographic feature of the landscape.

The possibility of reaching all different islands in the landscape through the use of mirror quintic monodromy transformations, is connected with the unresolved problem of the finiteness of the index of the monodromy subgroup in $Sp(4, \mathbb{Z})$. Our analysis has shown that there exists continuous transformations that connect minima in infinite series if we make use of geometric transitions into a moduli space of larger dimension. The question of whether such transformations can be found in the original setting remains unanswered.

The picture of the interconnections between different models, that we have exploited in order to investigate the series of minima, represents an interesting result in itself. To our knowledge, the complete relation between two models related by geometric transitions has not been made explicit before at the level we do it here. We were able to find the precise map between the complex structure moduli spaces of the mirror quintic and the manifold $\mathcal{M}_{(86,2)}$ by analysing the behavior of the periods of the latter. This embedding is fully explicit, including the reduction of the monodromy transformations.

The analysis was performed neglecting issues regarding Kähler moduli and backreaction on the geometry, but took into account, even if in some cases at a speculative level, the presence of all possible flux configurations. On the side of the manifold $\mathcal{M}_{(86,2)}$, we are in full control of the scalar potential of the theory, and we can effectively study its behavior in certain limits. When we relate it to the potential of the mirror quintic, though, issues regarding the behavior of the fluxes arise.

The geometric transition between the two manifolds involves the shrinking of 16 three-cycles on the $\mathcal{M}_{(86,2)}$ side and the blowing up of the same number of two-cycles on the mirror quintic one. If no flux pierces any of these cycles, we have a complete and fully understood picture of the result of the transformation on the mirror quintic side. If we instead have fluxes piercing the shrinking cycles and/or the three-cycle that intersect them, then the picture is more complicated.

Having fluxes only on the shrinking cycles will lead to the appearance of D5-branes or NS5-branes wrapping the blown-up two-cycles on the mirror quintic side [42, 43]. If the flux pierces only the intersecting cycle, the outcome is less clear. Our results show that, at the mirror quintic locus in the complex structure moduli space of $\mathcal{M}_{(86,2)}$, the contribution to the (super)potential depending on those fluxes vanishes. Therefore, the transition is not hindered by having such flux. In both the above cases we have no change in the tadpole condition on the mirror quintic, so no D3-branes need to be nucleated in the transition.

Instead if the fluxes pierce both the shrinking cycles and the intersecting one, the tadpole condition will in general change with the nucleation of D3-branes as a result. It is not clear exactly what happens in the present compact case, but it is possible that a similar nucleation of D3-branes as the one happening in the Klebanov–Strassler setup will take place.

Different minima imply the presence of domain walls separating them in space. As analyzed in [14], the appearance of different islands for the mirror quintic leads to the conjecture that two different kinds of domain walls exist. One kind separates fluxes

that could be connected through a monodromy transformation for which a profile depending on the complex structure moduli can be derived. The other separates islands that cannot be continuously connected and therefore corresponds to branes.

In the setup of the present work, we make use of the embedding of the mirror quintic moduli space into the moduli space of $\mathcal{M}_{(86,2)}$ in order to derive profiles of a larger set of domain walls. What happens is that the moduli change when we cross a domain wall; we leave the mirror quintic moduli space through a geometric transition to the $\mathcal{M}_{(86,2)}$, and at the end we come back through another geometric transition to the mirror quintic. With no fluxes on the shrinking cycle we have complete control over the domain wall. When there is a flux through the shrinking cycle the situation is less clear. If the potential barrier at the geometric transition generated by the flux through the shrinking cycle is regulated by stringy corrections, then one can expect to obtain domain walls separating volumes of space time with different number of five-branes.

What happens to fluxes through a geometric transition is a very interesting open question. It leaves open new possibilities for finding minima and analysing domain walls through the new terms in the scalar potential generated by the presence of the fluxes. It clearly deserves further investigation, together with the analysis of the dynamics of Kähler moduli and backreaction on the geometry, in order to have a complete picture.

Our results and the techniques employed lead to interesting possibilities for future research. First of all, the topographic features of the landscape that we have found (namely long series of closely spaced vacua) represent a good setting for chain inflation [54, 55] and for the resonance tunneling [56]. The techniques we have employed, and further refinements of them, give hope to obtain a quantitative understanding of these phenomena. The same techniques can also be used for quantitative study of the domain walls between different minima.

Acknowledgments

The work was supported by the Swedish Research Council (VR). We would like to thank Shamit Kachru and Maximilian Kreuzer for useful discussions.

A Notation and numerics

This appendix explains our notational conventions for the Calabi-Yau geometry and how the numerical computations of the scalar potential are performed.

A.1 Geometry

Denote by \mathcal{M} a Calabi–Yau manifold with complex structure moduli space M . The periods of \mathcal{M} are the “holomorphic volumes” of a basis of 3-cycles:

$$\Pi_I = \oint_{C_I} \Omega = \oint_{\mathcal{M}} C_I \wedge \Omega. \quad (106)$$

Here Ω is the holomorphic 3-form and C_I denotes a basis of $H_3(\mathcal{M})$. Note that C_I denotes both the cycles and their Poincaré duals. The index I runs from 1 to $2h^{1,2}(\mathcal{M}) + 2 \equiv N$. The intersection matrix $Q = (Q_{IJ})$ is defined as

$$Q_{IJ} = \oint_{C_I} C_J = \oint_{\mathcal{M}} C_I \wedge C_J. \quad (107)$$

We will call Q_{IJ} canonical if the cycles C_I, C_J intersect only pairwise, with intersection number ± 1 .

Denoting the cycles corresponding to the Π -basis of section 4 by C_I , the cycle that vanishes on the mirror quintic locus is C_5 and its dual is C_6 . We also refer to these cycles by the conventional A and B . The cycle that shrinks at the locus intersecting the mirror quintic moduli space in the conifold point of the latter is C_1 . It is intersected by the cycle C_4 .

It is customary and convenient to collect the periods into a vector

$$\Pi(\phi) = \begin{pmatrix} \Pi_1(\phi) \\ \Pi_2(\phi) \\ \vdots \\ \Pi_N(\phi) \end{pmatrix}, \quad (108)$$

where ϕ is an $(N/2 - 1)$ -dimensional (complex) coordinate on M .

The periods are subject to monodromies:

$$\Pi \rightarrow T \cdot \Pi, \quad (109)$$

where T is a matrix that preserves the symplectic structure Q . All possible monodromy matrices constitute a subgroup of $Sp(N, \mathbb{Z})$.

In our example $\mathcal{M}_{(86,2)}$ we choose a notation for the monodromies that coincides with the one used in [14] when reducing to the mirror quintic.²⁵ Thus T_0 corresponds to encircling $z_2 = 0$ always staying at the locus $z_1 = 0$.

A.2 The scalar potential

Given the periods one can compute the $\mathcal{N} = 1$ scalar potential for given flux quanta. The standard form of the scalar potential is

$$V(\phi, \tau) = e^K \left(g^{i\bar{j}} D_i W D_{\bar{j}} \bar{W} + g^{\tau\bar{\tau}} D_\tau W D_{\bar{\tau}} \bar{W} + g^{\rho\bar{\rho}} D_\rho W D_{\bar{\rho}} \bar{W} - 3|W|^2 \right), \quad (110)$$

²⁵However, to get a clearer notation, we index the monodromy matrices as T_i instead of $T[i]$ in this paper.

where, as usual, the matrix $g^{A\bar{B}} = (\partial_A \partial_{\bar{B}} K)^{-1}$ and $D_A = \partial_A + \partial_A K$. In this paper we focus on the no-scale case, where the contributions of $g^{\rho\bar{\rho}} D_\rho W D_{\bar{\rho}} \bar{W}$ and $-3|W|^2$ cancel:

$$V(\phi, \tau) = e^K (g^{i\bar{j}} D_i W D_{\bar{j}} \bar{W} + g^{\tau\bar{\tau}} D_\tau W D_{\bar{\tau}} \bar{W}). \quad (111)$$

To compute V all that is needed are expressions for the superpotential W and the Kähler potential K . We collect the flux quanta in row vectors²⁶ F and H according to $F_{(3)} = -\sum_I F_I C_I = -F \cdot C$ and $H_{(3)} = -\sum_I H_I C_I = -H \cdot C$. The superpotential is then given by

$$W = \int_{\mathcal{M}} \Omega \wedge (F_{(3)} - \tau H_{(3)}) = F \cdot \Pi - \tau H \cdot \Pi. \quad (112)$$

The Kähler potential is

$$K = -\ln(-i(\tau - \bar{\tau})) + K_{\text{cs}}(\phi, \bar{\phi}) - 3\ln(-i(\rho - \bar{\rho})). \quad (113)$$

K_{cs} is the Kähler potential for the complex structure moduli, and is given by

$$K_{\text{cs}} = -\ln \left(-i \int_{\mathcal{M}} e^{-4A} \Omega \wedge \bar{\Omega} \right). \quad (114)$$

Neglecting warping we have

$$K_{\text{cs}} = -\ln(-i\Pi \cdot Q^{-1} \cdot \Pi). \quad (115)$$

Using (112), (113) and (115) the scalar potential can be computed numerically once the periods and their derivatives are known.

A.3 Numerics on the mirror quintic

Let us use the coordinate $z = 5^5 z_2$ on the mirror quintic moduli space. To find minima of the scalar potential (111) on the mirror quintic for given fluxes, we start by solving for τ in the equation

$$\partial_\tau V(z, \tau) = 0 \quad (116)$$

to obtain²⁷ $V(z) = V(z, \tau(z))$. This function has a minimum exactly when $V(z, \tau)$ does. We compute the periods $\Pi_1(z), \dots, \Pi_4(z)$ and their derivatives on a grid in moduli space M using the *Maple* software package. We use the Meijer-G functions

²⁶Note that, with this notation, having e.g., $F_1 \neq 0$ does not mean that we have fluxes around C_1 . Instead it means having fluxes through the intersecting cycle C_4 . More generally $\int_{C_I} F_{(3)} = -\int_{C_I} \sum_J F_J C_J = \sum_J F_J Q_{JI} = (F \cdot Q)_I \neq F_I$.

²⁷We suppress the dependence of V and τ on \bar{z} to simplify the notation.

as explained in [57]. We repeat the formulas here for the reader's convenience. In *Maple* notation we define

$$\begin{aligned}
U_0^-(z) &= \text{MeijerG}([4/5, 3/5, 2/5, 1/5], [], [[0], [0, 0, 0]], -z) \\
U_1^-(z) &= \frac{1}{2\pi i} \text{MeijerG}([4/5, 3/5, 2/5, 1/5], [], [[0, 0], [0, 0]], z) \\
U_2^-(z) &= \frac{1}{(2\pi i)^2} \text{MeijerG}([4/5, 3/5, 2/5, 1/5], [], [[0, 0, 0], [0]], -z) \\
U_3^-(z) &= \frac{1}{(2\pi i)^3} \text{MeijerG}([4/5, 3/5, 2/5, 1/5], [], [[0, 0, 0, 0], []], z),
\end{aligned} \tag{117}$$

and

$$\begin{aligned}
U_0^+(z) &= U_0^-(z) \\
U_1^+(z) &= U_1^-(z) + U_0^-(z) \\
U_2^+(z) &= U_2^-(z) \\
U_3^+(z) &= U_3^-(z) + U_2^-(z).
\end{aligned} \tag{118}$$

A basis $U_j(z)$ for the mirror quintic periods is then defined by $U_j(z) = U_j^-(z)$ for $\text{Im}(z) < 0$ and $U_j(z) = U_j^+(z)$ for $\text{Im}(z) > 0$. The basis U_j is related to the basis Π by $\Pi = LU$ with

$$L = \frac{8i\pi^3}{125} \begin{pmatrix} 0 & 5 & 0 & 5 \\ 0 & 3 & -5 & 0 \\ 0 & -1 & 0 & 0 \\ 1 & 0 & 0 & 0 \end{pmatrix}. \tag{119}$$

The derivatives of the periods $\partial_z \Pi$ needed for computing e.g. $D_z W = \partial_z W + (\partial_z K)W$ and $K_{z\bar{z}}$ can also be obtained as Meijer-G functions and calculated in the same way.

Equipped with $\Pi(z)$ and $\partial_z \Pi(z)$ on a grid in moduli space we use *Matlab* to efficiently compute the potential for a large number of flux vectors. In this way the example of section 6 was found.

References

- [1] P. Candelas, G. T. Horowitz, A. Strominger and E. Witten, "Vacuum Configurations For Superstrings," Nucl. Phys. B **258** (1985) 46.
- [2] M. Grana, "Flux compactifications in string theory: A comprehensive review," Phys. Rept. **423**, 91 (2006) [arXiv:hep-th/0509003].
- [3] O. DeWolfe and S. B. Giddings, "Scales and hierarchies in warped compactifications and brane worlds," Phys. Rev. D **67**, 066008 (2003) [arXiv:hep-th/0208123].
- [4] S. Kachru, R. Kallosh, A. Linde and S. P. Trivedi, "De Sitter vacua in string theory," Phys. Rev. D **68**, 046005 (2003) [arXiv:hep-th/0301240].

- [5] V. Balasubramanian, P. Berglund, J. P. Conlon and F. Quevedo, “Systematics of moduli stabilisation in Calabi-Yau flux compactifications,” *JHEP* **0503**, 007 (2005) [arXiv:hep-th/0502058].
- [6] L. Susskind, “The anthropic landscape of string theory,” arXiv:hep-th/0302219.
- [7] F. Denef and M. R. Douglas, “Computational complexity of the landscape. I,” arXiv:hep-th/0602072.
- [8] B. S. Acharya and M. R. Douglas, “A finite landscape?,” arXiv:hep-th/0606212.
- [9] J. D. Bryngelson, J. N. Onuchic, N. D. Socci, P. G. Wolynes, ”Funnels, Pathways and the Energy Landscape of Protein Folding: A Synthesis”, *Proteins-Struct. Func. and Genetics.* 21 (1995) 167 arXiv:chem-ph/9411008
- [10] R. Bousso and J. Polchinski, “Quantization of four-form fluxes and dynamical neutralization of the cosmological constant,” *JHEP* **0006**, 006 (2000) [arXiv:hep-th/0004134].
- [11] A. Ceresole, G. Dall’Agata, A. Giryavets, R. Kallosh and A. Linde, “Domain walls, near-BPS bubbles, and probabilities in the landscape,” *Phys. Rev. D* **74** (2006) 086010 [arXiv:hep-th/0605266].
- [12] T. Clifton, A. Linde and N. Sivanandam, “Islands in the landscape,” *JHEP* **0702** (2007) 024 [arXiv:hep-th/0701083].
- [13] S. Sarangi, G. Shiu and B. Shlaer, “Rapid Tunneling and Percolation in the Landscape,” arXiv:0708.4375 [hep-th].
- [14] U. H. Danielsson, N. Johansson and M. Larfors, “The world next door: Results in landscape topography,” *JHEP* **0703**, 080 (2007) [arXiv:hep-th/0612222].
- [15] Yao-Han Chen, Yifan Yang, Noriko Yui, “Monodromy of Picard-Fuchs differential equations for Calabi-Yau threefolds,” arXiv:math.AG/0605675.
- [16] P. Green and T. Hubsch, “Calabi-Yau Manifolds As Complete Intersections In Products Of Complex Projective Spaces,” *Commun. Math. Phys.* **109** (1987) 99.
- [17] P. Candelas, P. S. Green and T. Hubsch, “Rolling Among Calabi-Yau Vacua,” *Nucl. Phys. B* **330**, 49 (1990).
- [18] B. R. Greene and M. R. Plesser, “Duality in Calabi-Yau moduli space,” *Nucl. Phys. B* **338**, 15 (1990).
- [19] P. Candelas, X. C. De La Ossa, P. S. Green and L. Parkes, “A pair of Calabi-Yau manifolds as an exactly soluble superconformal theory,” *Nucl. Phys. B* **359**, 21 (1991).

- [20] B. R. Greene, D. R. Morrison and A. Strominger, “Black hole condensation and the unification of string vacua,” Nucl. Phys. B **451**, 109 (1995) [arXiv:hep-th/9504145].
- [21] V. V. Batyrev, “Dual polyhedra and mirror symmetry for Calabi-Yau hypersurfaces in toric varieties,” J. Alg. Geom. **3**, 493 (1994).
- [22] M. Kreuzer, “Toric Geometry and Calabi-Yau Compactifications,” arXiv:hep-th/0612307.
- [23] D. A. Cox and S. Katz, “Mirror symmetry and algebraic geometry,” *Providence, USA: AMS (2000)*
- [24] B. R. Greene, “String theory on Calabi-Yau manifolds,” arXiv:hep-th/9702155.
- [25] W. Fulton, “Introduction to Toric Varieties,” Ann. of Math. Stud. 131, Princeton Univ. Press, Princeton, 1993.
- [26] K. Hori *et al.*, “Mirror symmetry,” Providence, USA: AMS (2003) 929 p.
- [27] V. V. Batyrev, I. Ciocan-Fontanine, B. Kim and D. van Straten, “Conifold Transitions and Mirror Symmetry for Calabi-Yau Complete Intersections in Grassmannians” [arXiv:alg-geom/9710022].
- [28] I.R. Shafarevic, *Basic Algebraic Geometry*, Springer-Verlag
- [29] L. Borisov, ”Towards the Mirror Symmetry for Calabi-Yau Complete intersections in Gorenstein Toric Fano Varieties”, [alg-geom/9310001]
- [30] V. V. Batyrev and L. A. Borisov, ”Dual Cones and Mirror Symmetry for Generalized Calabi-Yau Manifolds” [alg-geom/9402002]
- [31] V. V. Batyrev and L. A. Borisov, “On Calabi-Yau complete intersections in toric varieties,” arXiv:alg-geom/9412017.
- [32] A. Klemm, M. Kreuzer, E. Riegler and E. Scheidegger, “Topological string amplitudes, complete intersection Calabi-Yau spaces and threshold corrections,” JHEP **0505**, 023 (2005) [arXiv:hep-th/0410018].
- [33] M. Kreuzer and H. Skarke, “PALP: A Package for Analyzing Lattice Polytopes with Applications to Toric Geometry,” Comput.Phys.Commun. **157**, 87-106 (2004), arXiv:math/0204356 [math.NA].
- [34] P. Berglund and S. H. Katz, “Mirror symmetry constructions: A review,” arXiv:hep-th/9406008.
- [35] B. R. Greene, D. R. Morrison and C. Vafa, “A geometric realization of confinement,” Nucl. Phys. B **481**, 513 (1996) [arXiv:hep-th/9608039].

- [36] S. Hosono, A. Klemm, S. Theisen and S. T. Yau, “Mirror Symmetry, Mirror Map And Applications To Calabi-Yau Hypersurfaces,” *Commun. Math. Phys.* **167** (1995) 301 [arXiv:hep-th/9308122].
- [37] S. Hosono, A. Klemm, S. Theisen and S. T. Yau, “Mirror symmetry, mirror map and applications to complete intersection Calabi-Yau spaces,” *Nucl. Phys. B* **433** (1995) 501 [arXiv:hep-th/9406055].
- [38] S. Hosono, B. H. Lian and S. T. Yau, “Maximal Degeneracy Points of GKZ Systems,” arXiv:alg-geom/9603014.
- [39] S. Hosono, “Local mirror symmetry and type IIA monodromy of Calabi-Yau manifolds,” *Adv. Theor. Math. Phys.* **4** (2000) 335 [arXiv:hep-th/0007071].
- [40] M. Abramowitz and I. A. Stegun, “Handbook of Mathematical Functions with Formulas, Graphs, and Mathematical Tables”, Dover, New York, NY, USA (1972).
- [41] V. Arnold, A. Gusein-Zade and A. Varchenko, *Singularities of Differentiable Maps I, II*, Birkhäuser 1985.
- [42] R. Gopakumar and C. Vafa, “On the gauge theory/geometry correspondence,” *Adv. Theor. Math. Phys.* **3**, 1415 (1999) [arXiv:hep-th/9811131].
- [43] C. Vafa, “Superstrings and topological strings at large N,” *J. Math. Phys.* **42**, 2798 (2001) [arXiv:hep-th/0008142].
- [44] E. Witten, “Branes and the dynamics of QCD,” *Nucl. Phys. B* **507**, 658 (1997) [arXiv:hep-th/9706109].
- [45] S. Kachru, S. H. Katz, A. E. Lawrence and J. McGreevy, “Open string instantons and superpotentials,” *Phys. Rev. D* **62**, 026001 (2000) [arXiv:hep-th/9912151].
- [46] S. Kachru, S. H. Katz, A. E. Lawrence and J. McGreevy, “Mirror symmetry for open strings,” *Phys. Rev. D* **62**, 126005 (2000) [arXiv:hep-th/0006047].
- [47] M. Aganagic and C. Vafa, “Mirror symmetry, D-branes and counting holomorphic discs,” arXiv:hep-th/0012041.
- [48] P. Mayr, “Aspects of N=1 mirror symmetry,” *Prepared for 10th International Conference on Supersymmetry and Unification of Fundamental Interactions (SUSY02), Hamburg, Germany, 17-23 Jun 2002*
- [49] W. y. Chuang, S. Kachru and A. Tomasiello, “Complex / symplectic mirrors,” *Commun. Math. Phys.* **274**, 775 (2007) [arXiv:hep-th/0510042].
- [50] M. Aganagic, C. Beem and S. Kachru, “Geometric Transitions and Dynamical SUSY Breaking,” arXiv:0709.4277 [hep-th].

- [51] I. R. Klebanov and M. J. Strassler, “Supergravity and a confining gauge theory: Duality cascades and chiSB-resolution of naked singularities,” *JHEP* **0008**, 052 (2000) [arXiv:hep-th/0007191].
- [52] S. B. Giddings, “The fate of four dimensions,” *Phys. Rev. D* **68**, 026006 (2003) [arXiv:hep-th/0303031].
- [53] S. B. Giddings, S. Kachru and J. Polchinski, “Hierarchies from fluxes in string compactifications,” *Phys. Rev. D* **66** (2002) 106006 [arXiv:hep-th/0105097].
- [54] K. Freese and D. Spolyar, “Chain inflation: ‘Bubble bubble toil and trouble’,” *JCAP* **0507** (2005) 007 [arXiv:hep-ph/0412145].
- [55] K. Freese, J. T. Liu and D. Spolyar, “Chain inflation via rapid tunneling in the landscape,” arXiv:hep-th/0612056.
- [56] S. H. Henry Tye, “A new view of the cosmic landscape,” arXiv:hep-th/0611148.
- [57] F. Denef, B. R. Greene and M. Raugas, “Split attractor flows and the spectrum of BPS D-branes on the quintic,” *JHEP* **0105** (2001) 012 [arXiv:hep-th/0101135].